Chemo-specific Designs for the Enumeration of Circulating Tumor Cells: Advances in Liquid Biopsy

Balram Singh[†b], Smriti Arora[†b], Alain D'Souza[b], Narendra Kale[b], Gourishankar Aland[b], Atul Bharde[b,c], Mohiuddin Quadir[d], Marcelo Calderón[e,f], Pankaj Chaturvedi[g], Jayant Khandare [a,b*]

Affiliations:

[a] School of Pharmacy, Dr. Vishwanath Karad Maharashtra Institute of Technology-World Peace University, Kothrud, Pune 411038, India

[b] Actorius Innovations and Research Pvt. Ltd., Pune, 411057 India

[c] Current: Dept. of Microbiology, Savitribai Phule Pune University, Pune, 411007 India

[d] Department of Coatings and Polymeric Materials, North Dakota State University, Fargo, ND, 58108, USA

[e] POLYMAT and Applied Chemistry Department, Faculty of Chemistry, University of the Basque Country UPV/EHU, Paseo Manuel de Lardizabal 3, 20018 Donostia-San Sebastián, Spain

[f] IKERBASQUE, Basque Foundation for Science, 48013 Bilbao, Spain

[g] Department of Head and Neck Surgical Oncology, Tata Memorial Hospital, Mumbai, 400012 India

[†] Authors contribute equally

*Corresponding author: jayant.khandare@mippune.edu.in

Keywords: Circulating Tumor Cells (CTCs), chemo-specific targeting materials, CTC-specific tumor biomarkers, cancer detection

Abstract

Advanced materials and chemo-specific designs at the nano/micrometer-scale have ensured revolutionary progress in next-generation biologically and clinically relevant technologies. For example, isolating a rare population of cells, like circulating tumor cells (CTCs) from the blood amongst billion of other blood cells, is one of the most complex scientific challenges in cancer diagnostics. The chemical tunability to achieve this degree of exceptional specificity for extra-cellular biomarker interactions demands the utility of advanced entities and multistep reactions both in solution and the insoluble state. Thus, this review delineates the chemo-specific substrates, chemical methods, and structure-activity relationship (SAR) of chemical platforms used for isolation and enumeration of CTCs in advancing the relevance of liquid biopsy in cancer diagnostics and disease management. We highlight the synthesis of cell-specific, tumor biomarker-based, chemo-specific substrates utilizing functionalized linkers through chemistry-based conjugation strategies. These nano/micro substrates' capacity to enhance the cell interaction specificity and efficiency with the targeted tumor cells is detailed. Furthermore, this review accounts for the importance of CTC capture and other downstream processes involving genotypic and phenotypic CTC analysis in real-time for detection of early onset of metastases progression, chemotherapy treatment response, and in monitoring progression free-survival (PFS), disease-free survival (DFS), and eventually overall survival (OS) in cancer patients.

1. Introduction

Various advanced materials have been proposed for biological and clinical applications in theranostics, imaging, and diagnostics.[1-10] The synthetic strategies in designing such advanced materials involve the prodigious combination of coordination, conjugation, and biorthogonal reactions; hybridizing both chemical and biological entities or substrates, such as carbon allotropes, linear and hyperbranched polymers, iron oxide nanoparticles (FeNPs), silver nanoparticles (AgNP), gold nanoparticles (AuNP), silicates, proteins, antibodies, etc. (**Figure 1**).[1-4, 9] The synthetic strategies adopted to design such materials impart the desired structure-activity relationships (SAR), and enable control over the physicochemical traits including, architecture, micro/nano size, surface charge, branching, spatial control, stimuli sensitivity, medium dispersibility, etc.[11-17] Thus, the capacity to control the attributes mentioned above have improved the specificity and efficiency for various biological applications including infectious diseases, blood disorders, and detection of cancer both at phenotype and genotype levels.[18-20]

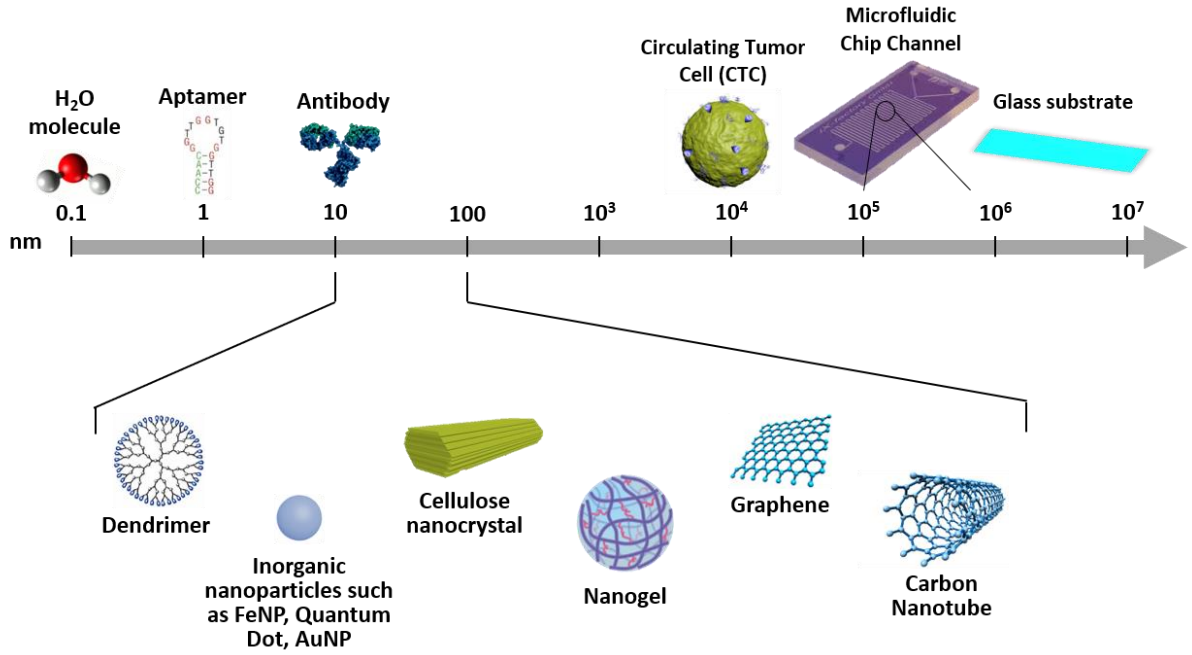

Figure 1: Length scale showing the size of nano/micro substrates compared to biochemical targeting ligands and circulating tumor cells (CTCs). The characteristic size of nano/micro-substrates places them in between the targeting ligands and CTCs.

Metabolic disorders in developing countries and cancer incidences in developed countries have been rising at an alarming rate. In particular, cancer is responsible for one in six deaths making it the second most common cause globally.[21] Thus, cancer disease management stresses a multidisciplinary scientific approach involving cellular, proteomic, and genomic-based diagnostic capacities combine into a single platform due to tumor heterogenicity and longitudinal information of the disease. Such a platform will improve clinical disease status determination, in addition, act as an enabling technology for treatment monitoring responses and outcome.[21] Furthermore, the disease burden has been enhanced socio-economically. It is further propelled by rapid population growth, ageing societies, lifestyles, and increasing commercial interests.[22,

[23] In 2018, 18.1 million cancer incidences and 9.6 million cancer-related deaths were reported worldwide.[22, 23] Additionally, unhealthy lifestyles resulting from smoked or chewed tobacco use, alcohol abuse, and improper diet are propelling the prevalence of head and neck cancers globally, especially within Asian population where access to advanced healthcare may not be readily available or affordable.[24] Unfortunately, 90% of cancer-related deaths are attributed to metastasis, and only 10% are related to primary tumorigenesis.[25, 26]

Metastasis involves extravasation and invasion of distant organ sites, triggered by CTCs through dissemination and intravasation from a primary tumor site, transport via the peripheral blood system, and colonization and formation of micro-metastatic sites at distant organs.[27] The significance of CTCs as an independent risk factor in several epithelial origin cancer types, termed carcinomas, has been identified in over 400 clinical studies including, breast cancer, colorectal cancer, prostate cancer, lung cancer, and hepatocellular carcinomas.[28-32] The incidences and the types of cancers across the globe demarcates the regional socio-economical strata. For instance, Head and Neck cancers (HNC) prevalence in India is the highest in the world due to various factors, including tobacco use. A recent study by Khandare et al. showed that among the Indian population, CTC presence correlates with numerous clinicopathological parameters in HNC, particularly oral squamous cell carcinomas, and therefore, the use of CTC numbers as a viable marker for establishing clinical staging in HNC patients (**Figure 2c**).[33, 34]

Consequently, CTCs represent a central biomarker isolated from peripheral blood through non-invasive blood sampling, referred to as 'liquid biopsy.' Thus, CTCs offer a higher prognostic value for the prediction of cancer progression and monitoring therapeutic responses.[32, 35] Detection, identification, and molecular characterization of CTCs thus play a pivotal role in unprecedented insights into the metastatic process. The potential clinical benefits associated with CTC detection and characterization and the ever-evolving understanding of material chemistry and tumor biology have been utilized to design various platforms for the static and dynamic enrichment of CTCs.

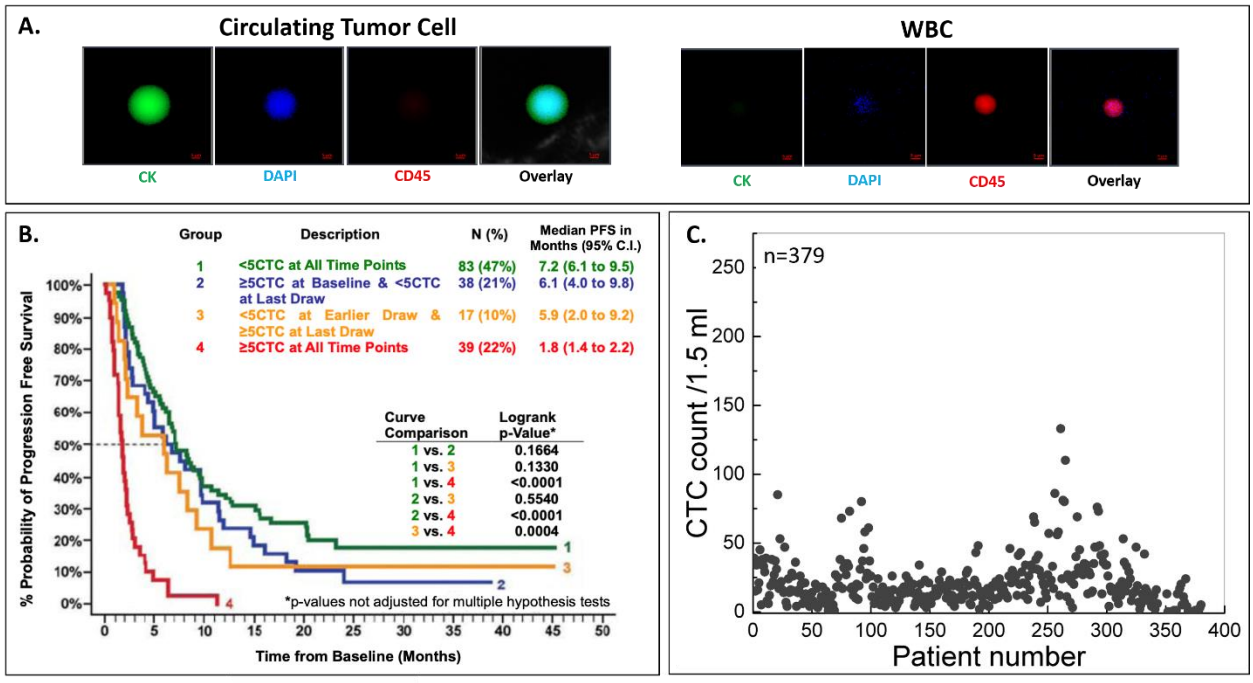

Figure 2: Clinical significance of CTCs in carcinomas. **A)** Representative images of CTC and white blood cell (WBC) isolated from a cancer patient blood sample. Immunostaining performed with FITC labelled anti-cytokeratin antibody, and AlexaFluor 555 labelled anti-CD45 antibody. 4',6-diamidino-2-phenylindole (DAPI) was used for nuclear counterstaining of CTC and WBC. CTCs indicate positive CK staining and negative CD45 staining. WBCs are positive for CD45 and negative for CK. Both cells are positive for nuclear stain. Scale bars represent 5 μm; **B)** Reduction in CTC number below 5 after therapy initiation predicts more prolonged progression-free survival (PFS), whereas an increase in CTC count to 5 or higher predicts shorter PFS in metastatic breast cancer (mBC) patients. The PFS graph indicates that patients with ≥ 5 CTCs at all time points (Group 4) showed the least median PFS, which was significantly decreased compared to Groups 3, 2, and 1, respectively.[36] **C)** Clinical correlation of CTCs as a blood marker of disease progression in Indian HNC patients. CTC distribution of 379 Head and Neck Squamous Cell Carcinoma (HNSCC) patients. The mean CTC number distribution is 21. Correlation of CTC presence and clinicopathological disease parameters implicates the use of CTCs in establishing clinical staging in HNC patients.[33, 37]

Role of circulating tumor cells in cancer metastasis

Primary solid tumors are known to shed about 1 million CTCs per gram of tumor mass daily.[29-31] However, amongst other billion blood cells, the occurrence of CTCs is extremely low (1 CTC per 10^7 leukocytes per ml of blood), thus making them extremely rare.[32, 35] While disseminating from the primary tumor site and entering into blood circulation, CTCs undergo both genotypic and phenotypic changes through a process known as epithelial-mesenchymal transition (EMT).[38] Once in the circulatory system, CTCs exhibit varying phenotypic characteristics, namely, stemness (i.e., tumor-initiating properties), epithelial (i.e., adhesion), and mesenchymal (i.e., migration and invasion) properties. After that, CTCs tend to aggregate (up to > 100 cancer cells) along with different cell types, that may include immune cells, platelets, and cancer-associated fibroblasts. These extremely rare CTC clusters have aggressive metastatic potential estimated to be 23-50 times higher than single CTCs.[32, 39] Compared to single CTCs, CTC clusters have shorter circulation half-life. Also, the larger size of the cluster as compared to a single CTC is reported to enhance their rapid entrapment within blood capillaries of distant organs, where they may extravasate and activate metastatic growth under tumor favorable tissue microenvironments.[32, 39]

From the standpoint of survival and diagnosis, CTCs undergo unfavorable exposure in the bloodstream due to shear force (physical stress), anoikis, immune surveillance, apoptosis, and lack of growth factors. As a result, <0.01% of CTCs are known to survive and extravasate at favorable distant sites to seed secondary tumor growth.[40] The extravasated cells must undergo a reversal to their prior epithelial phenotype by reverse EMT - the mesenchymal-epithelial transition (MET) to activate metastasis at the distant organs.[28] Together, EMT and MET phases represent crucial transitory stages of cancer cells that result in heterogeneity of CTCs during the metastatic cascade. All such transitions correlate in real-time with favorable or unfavorable disease prognosis directly implying the PFS, DFS, and OS of the cancer patient (**Figure 2b**).

Approaches and challenges in CTC isolation technologies.

In 1869, Ashworth first described CTCs in the blood of a metastatic cancer patient. To date, a variety of strategies involving either biophysical or biochemical approaches have been developed

for the isolation of CTCs.[41] Biophysical-based methods depend on the transformations in the physical properties of CTCs paralleled to normal blood cells, including cell size, deformability, and density. Size-based filtration and density gradient centrifugation are two typical established biophysical methods used for CTC isolation and enrichment. Conversely, biochemical based approaches involve selective CTC isolation by immunoaffinity capture of unique cancer-specific biomarkers such as Epithelial Cell Adhesion Molecule (EpCAM), Human Epidermal Growth Factor Receptor 2 (HER2), Folic Acid Receptor (FR), Transferrin Receptor (TfR) that are overexpressed on the CTCs' surface. Positive identification of CTCs may be achieved by fluorescence microscopy using differential fluorescent antibodies to detect the presence of Cytokeratins (CK) (e.g., CK8, 18, 19, etc.), which are overexpressed in tumor cells, within nucleated cells (positive for nuclear counterstain DAPI) and for the absence of CD45 - a leukocyte surface biomarker. An event is positively confirmed as a circulating tumor cell when it exhibits tumor cell morphology and an $EpCAM^+$, CK^+, $DAPI^+$, and $CD45^-$ phenotype **(Figure 2a, Figure 3).**[42]

However, low numbers in blood and high heterogeneity are significant challenges associated with efficient isolation and characterization of CTCs. There occurs variability in size, shape, deformability, surface expression of cell surface tumor-specific biomarkers, etc. across and within CTC populations of diverse cancer subtypes, in different cancer patient, and at various disease stage time point.[43] For cancer metastasis, studies at the cellular, proteomic, and genetic levels demand the isolation of CTCs in high numbers using platforms capable of higher specificity and efficiency. These limitations can be overcome by employing CTC enrichment methods with higher specificity and minimizing contaminating normal hematopoietic cell fractions, thereby consequential in an increased number of enriched CTCs.

Broadly, these methods can be classified as i) Positive enrichment, which captures the target CTC cells and elutes other blood components such as clinically validated anti-epithelial cell adhesion antibody (anti-EpCAM) platforms, and ii) Negative enrichment, which captures the non-target normal blood cells (viz. erythrocytes (RBCs), leukocytes (WBCs), platelets, etc.) and elutes the target cell (i.e., CTCs). Positive enrichment technologies have many advantages, such as shorter CTC enrichment processes and retrieval of intact CTCs with minimal to no damage to cellular properties. Concomitantly, one of the significant limitations of approaches using negative enrichment of CTCs is the requirement of a considerable variety of antibodies required to eliminate normal hematopoietic constituents, thereby making the process expensive and also yielding low purity and specificity in the eluted CTC fraction, thus putting it beyond the scope of this review.[44]

Considering the critical challenges encountered in developing CTC isolation technologies, positive enrichment approaches utilizing nano/micro substrates conjugated to tumor-specific biomarkers have emerged as a predominant CTC isolation technique. Therefore, this review emphasizes the positive chemo-based CTC enrichment approaches and highlight the advances in chemistry design interface of various CTC capturing materials and its effect on the specificity and efficiency of CTC isolation and enumeration. The primary focus will describe the existing multi-component materials involving different nano/micro-based substrates conjugated to cell surface biomarkers in other spatial arrangements. In subsequent sections, we review the chemistry of dynamic systems and technologies for CTC isolation and detection. We also briefly describe the material design for the post-capture release of CTCs, which could be further useful for downstream analysis at the cellular, proteomic, and genomic levels.

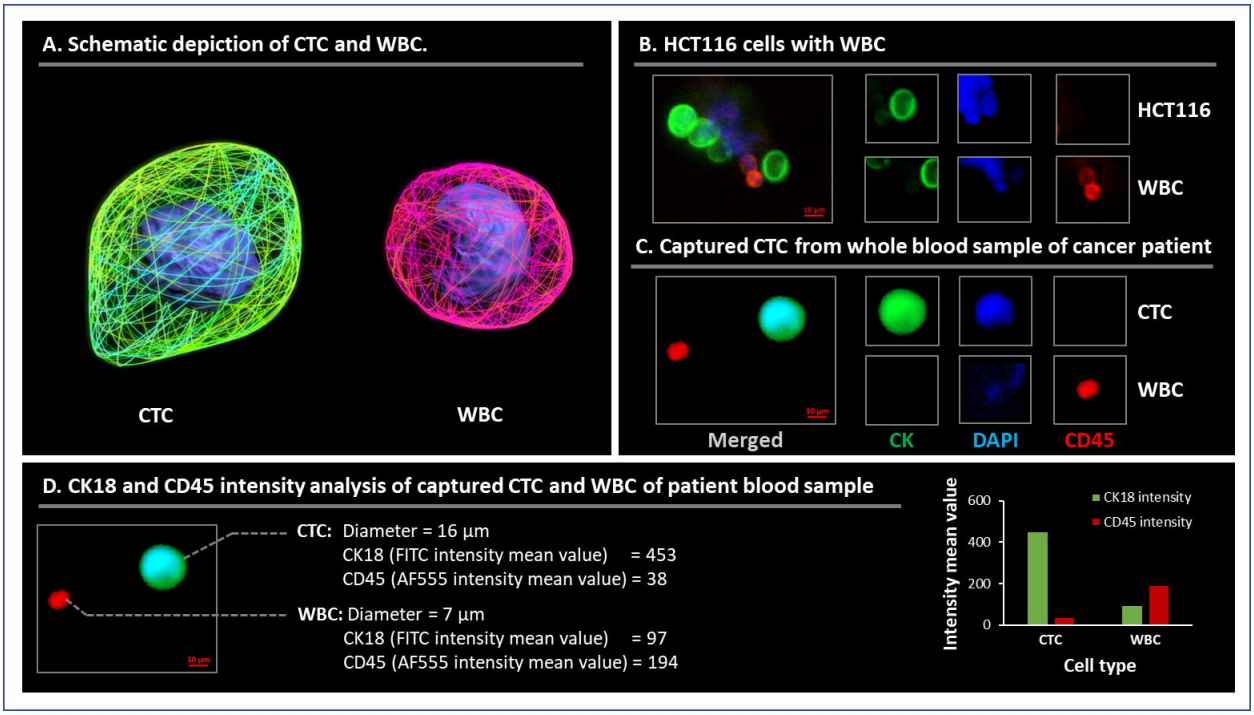

Figure 3: Differentiation characteristics between CTCs and WBCs. **A)** Schematic figure of a CTC and WBC illustrating CTC-specific cytoplasmic, overexpressed CK proteins (green), WBC surface-expressed leukocyte specific antigen-CD45 (red), and nucleus (blue). **B)** Spiked blood sample containing HCT116 colorectal carcinoma cell line, depicting characteristic CK and nuclear staining patterns using FITC-labelled anti-CK antibody and DAPI. WBCs stain positive for CD45 and nucleus (AlexaFluor555 labelled anti-CD45 antibody) but are negative for CK. **C)** Cancer patient blood sample with $CK^{+}DAPI^{+}CD45^{-}$ CTCs and $CD45^{+}DAPI^{+}CK^{-}$ WBCs. **D)** Size and immunofluorescence intensity differentiation of CTCs depicting larger cell diameter and higher CK18 and lower CD45 fluorescence intensity mean values (IMV) than WBCs. The graph represents IMV differences of CK18 and CD45 between CTCs and WBCs. Scale bar represents 10 µm.

Genomic profiling of CTC and DNA as liquid biopsy tools for next-generation cancer detection

Over the last couple of decades, a vast volume of research has highlighted the clinical utility of CTCs prognostic markers and a vital factor in monitoring cancer progression. However, CTC's real potential for personalized cancer disease management can be realized through its molecular and genomic characterization. This is because genomic profiling of CTCs can non-invasively recapitulate the primary and metastatic tumor constitution, which otherwise is not available from the tissue biopsy due to highly variable clinical behavior of the same type of cancer in different patients. CTC analysis at a molecular and genomic level can provide a plethora of information (**Figure 4**) such as cancer marker heterogeneity among the CTC population, temporal variations in key metastatic regulators, presence, and changes in stem cell marker expression, and dynamic variation in the therapeutic target expression.[45, 46]

Similarly, molecular profiling of CTCs is extremely valuable to better understand the epithelial to mesenchymal transition, a hallmark process of metastatic spread of the disease. Recent efforts for CTC characterization at the molecular and genomic level highlight their role in personalized

cancer care. Gambhir et al. have demonstrated the development and clinical utility of a novel nano platform that integrated magnetic isolation of CTCs and a nanowell array to isolate and sort thousands of CTCs at the single-cell level. Through this platform, EGFR, telomerase reverse transcriptase (TERT), and MET mutations and expression profiles could be detected heterogeneously among CTC populations originating from non-small cell lung cancer (NSCLC).[47]
Recently, Wang et al. observed a clear mutational heterogeneity in CTCs isolated from different epithelial tumors indicating the mutation is extremely different from the primary tumor.[48] This observation enabled the authors to understand the genetic and mutational heterogeneity based on single and multiple gene mutations in CTCs and the primary tumor. Efforts are ongoing to understand bloodborne metastasis by profiling CTCs obtained from breast cancer patients. In a seminal study, Park et al. performed expression profile and genome-wide copy number analysis on breast cancer CTCs.[49] Surprisingly, the EpCAM expressing CTC population did not display a phenotype attributed to breast cancer stem cells. Further, most of the CTCs expressed estrogen receptor 1 (ESR1) compared to HER2, and their expression pattern showed considerable changes compared to cells of the primary tumor.
A recent clinical study involving the gene expression profile of CTCs was observed to be strongly correlated with the clinical outcome of head and neck cancer. Patients with CTCs were strongly expressing or downregulating PI3K, MET, EGFR, ALDH1, CD44, CD47, and CD274 genes significantly correlated with treatment resistance, locoregional recurrence, and PFS. Further, a subpopulation of cancer patients with CD274 expressing CTCs had better PFS compared to patients with CD274 negative CTCs.[50]
Genetic analysis of CTCs is equally useful to understand the therapeutic potential of certain treatment regimens. In a prospective study, molecular profiling of CTCs from melanoma patients receiving combinatorial immunotherapy suggested that patients with CTCs expressing mutated BRAF and β-catenin were at high risk of poor therapeutic outcome.[51] Recently, Pantel and co-workers performed in-depth characterization of CTCs obtained from breast cancer patients that showed high metastatic and tumorigenic properties. Genetic analysis on these CTCs indicated that the cells retained high estrogen receptor (ER) expression ability and maintained a similar copy number variation profile compared to primary tumors. Further, down-regulation of ER signaling was constitutively active, impartial of ligand accessibility in CTCs and cyclin-dependent kinase inhibitors strongly inhibited CTC growth when cultivated in vitro.[52]
In addition, the characterization of protein markers on CTCs is valuable in clinical settings and can be readily achieved by flow cytometry or fluorescence microscopy. For example, dual Ki67/PSA (prostate-specific antigen) staining in CTCs of prostate cancer patients demonstrated increasing proliferation index in patients progressing from responsive disease to a more refractory resistant form.[53] Similarly, dual staining for androgen-induced and suppressed prostate-specific membrane antigen (PSMA) clearly showed the heterogeneity in androgen signaling status within CTCs before and after hormonal therapy.[54] However, care must be taken for multiplexed protein markers analysis in CTCs, as faulty antibody calibration with respect to signal intensity, background levels of markers expressed in a hematopoietic subpopulation of other cells, and cross-reactivity of antibodies can easily skew the results. This could be one of the prudent reasons why genomic characterization for molecular profiling of CTCs is fetching more popularity.
Moreover, emerging novel liquid biopsies techniques and Next Generation Sequencing (NGS) has enabled mutational analysis and cancer disease profiling at the single CTC level, thereby providing

unparalleled insights into the tumor heterogenicity, offering crucial aid to the clinical decision-making process.

Use of label-free inertial microfluidics for efficient CTC capture without relying on EpCAM expression, combined with multiplexed targeted resequencing assays, such as the Illumina TruSeq® Amplicon - Cancer Panel that targets 48 cancer-related genes and 212 amplicons, has been highly efficient. It has enabled the genomic alteration analysis of CTCs from head and neck, gastrointestinal cancer patients, as well as blood-based molecular profiling in identifying actionable drug targets, monitoring drug resistance, and tracking tumor dynamics and tumor DNA.[55] The earliest FDA approval for using such tests as a cohort diagnostic tool in clinical decisions for NSCLC therapy was granted in 2016 to the Roche cobas® EGFR mutation test v2. The test is based on real-time PCR that detects 42 mutations in specific exons of the EGFR gene from plasma or solid tumor samples. By 2020, qualitative NGS-based, pan-tumor liquid biopsy tests, such as the Roche-developed FoundationOne®Liquid CDx, have been granted FDA approval, thus further accelerating precision cancer therapy decisions in certain types of prostate, lung, breast, and ovarian cancer patients. By providing comprehensive genomic profiling of about 300 cancer-associated genes and genomic signatures within tumor DNA, such multiplex diagnostic tests enable crucial treatment decisions for solid tumor management and treatment based on data obtained from liquid biopsies.[36, 56]

Nevertheless, cancer type-specific antibody panels may ultimately provide valuable information to monitor tumor progression status and guide therapeutic choices. Taken together, molecular and genomic profiling of CTCs establishes a unique biomarker and mechanism of cancer progression and treatment resistance. Indeed, CTC profiling can have high clinical utility as it provides seeming benefits over tissue biopsy, including non-invasive contact of serial monitoring. Further, genotyping of CTCs is likely to be useful for mutation-targeted therapies in the lung (EGF and ALK mutations), skin (BRAF mutation), colorectal (EGFR and BRAF mutation), and breast (PI3K and HER2 mutations) cancers.[57]

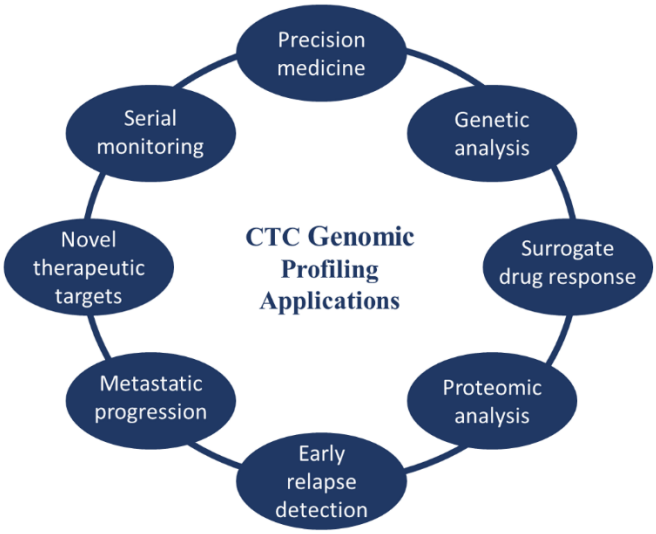

Figure 4: Biological and clinical utility of CTC molecular profiling. Genotypic and protein expression analysis of CTCs can be useful for various applications in cancer management.

Conversely, scientific progress has paved over the last decade, in terms of bio-marker based technologies, to detect blood-based, tumor-specific biomarkers; including CTCs and circulating DNAs cell-free DNA (cfDNA), circulating tumor DNA (ctDNA)). Tremendous efforts have been made to develop exceedingly sensitive liquid biopsy assays to detect and characterize minimal residual disease (MRD), specifically to determine the presence of tumor cells disseminated from the primary lesion to distant organs. Such tests are particularly critical in patients who display no clinical or radiological signatures of overt metastasis or residual tumor cells lingering after local therapy, ultimately leading to local disease recurrence. Hence, the detection of cfDNA, ctDNA, or CTCs years after treatment indicates the persistence of MRD.[58]

Liquid biopsy approaches based on detecting a small number of CTCs at primary cancer diagnosis predict an unfavorable prognosis. Therefore risk stratification strategies are even more applicable in such circumstances beyond the current approaches to tumor staging. Further, CTC and DNA characterization offers valuable insights into MRD's molecular evolution during tumor progression, with therapeutic implications to delay or even prevent metastatic relapse.[59] DNA evaluation critically using plasma genotyping ascertain the primary mutations, chromosome aberrations, insertions/deletions, amplifications, rearrangements, and aneuploidy. Overall, these signatures assist oncologists for longitudinal disease monitoring, the ability to capture tumor heterogenicity, and interventional trials to further enhance clinical decisions and care.[60]

Chemo-functionalities for enhanced cell-specific targeting in isolation and enumeration of CTCs.

Nanomaterials bearing cell-targeting ligands, such as an anti-EpCAM antibody, transferrin (Tf), luteinizing hormone-releasing hormone (LHRH), sialic acid, folic acid are known to promote cell-specific topographic interactions with their counter-receptors, thereby assisting the capture. Isolation, delivery, and recovery of cells.[61] Immobilization of targeting ligands (e.g., anti-EpCAM) on nanomaterials improves CTC recognition specificity significantly.[62] Furthermore, the nanomaterial's large surface to volume ratio endows high cellular binding affinity in the complex blood matrix. Manipulation of nanomaterials contributes to multiplex targeting and detection, which are crucial to approach the heterogeneous problem of CTCs.[63] Towards this, different types of nanostructured substrates, such as a magnetic nanoparticle, graphene, carbon nanotube (CNT), nanogel, cellulose nanocrystal, nanofiber, hyperbranched polymer, such as poly(amidoamine) dendrimer, and polyglycerol based platforms have been delineated (**Figure 1**).[8, 64-67] Moreover, some multi-component microfluidic substrates such as glass/polydimethylsiloxane (PDMS) assembly coupled to nanomaterial, further conjugated with CTC surface-specific markers have also been established as promising dynamic CTC isolation techniques (**Figure 5**).[68,69] Such microfluidic assemblies can attain maximal ligand-target interaction by controlling the residence of time of cancer cell-containing fluid.

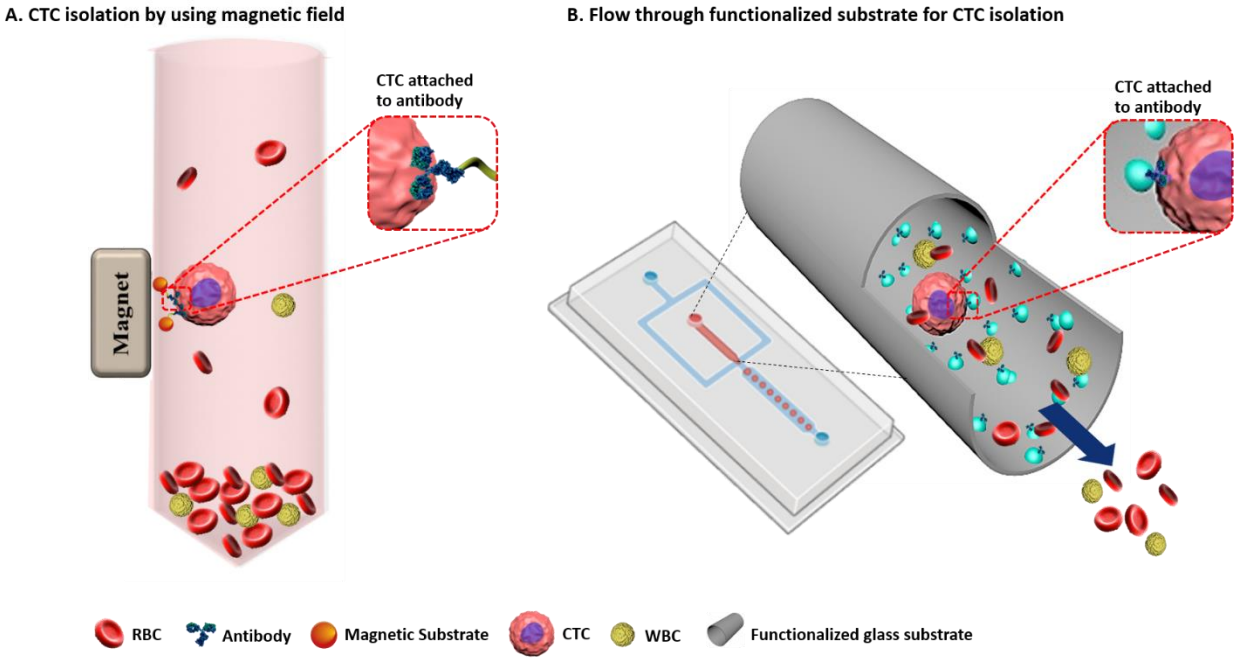

Figure 5: Schematics representing the two most widely used methodologies for CTC isolation, i.e., **A)** Static system: Immunomagnetic based CTC isolation; **B)** Dynamic flow-through system: Immuno-affinity-based CTC isolation.

A diversity of organic functional groups such as amine, carboxylic acid, aldehyde, thiol, alcohol, etc., can be introduced on nano-substrates during or post-synthesis to render the ensemble reactive and specific. These functionalities offer basic colloidal properties to the nano-substrates, offer increased biocompatibility, enable conjugation with linkers such as small organic molecules, polymers, macromolecules, and finally introduce active biological moieties such as antibodies, DNA, and proteins. Some of the nano-substrates functionalized with small molecules followed by conjugation to the antibody using the most commonly used carbodiimide coupling are illustrated in **Figure 6**.[70]

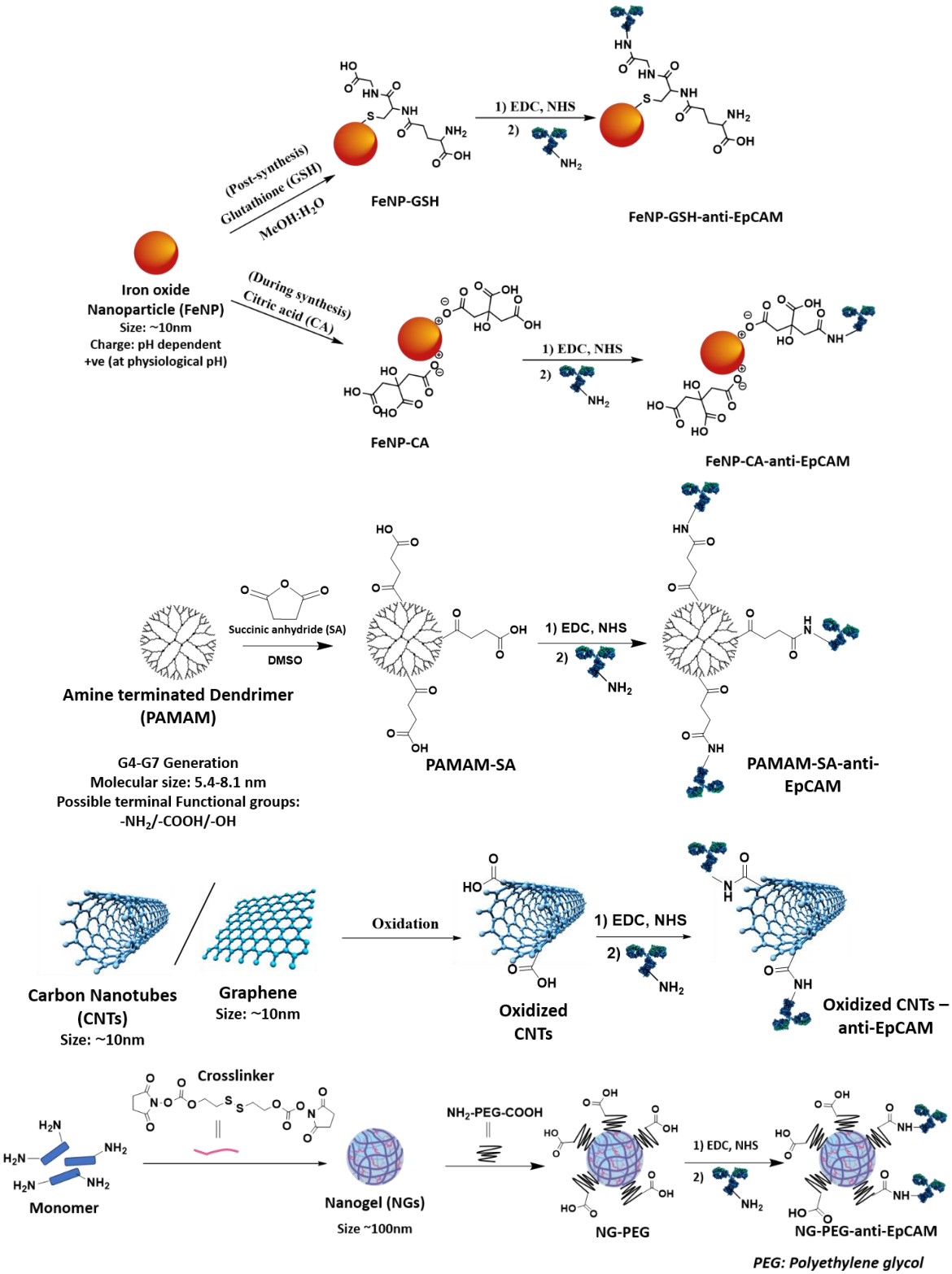

Figure 6: Schematic representation for the generation of reactive functionalities on the commonly used nano-substrates and linking targeting ligands for CTC capture and isolation. Acidic functional groups have been introduced onto the nano-substrates, followed by

conjugating anti-EpCAM by carbodiimde coupling using 1-Ethyl-3-(3-dimethylaminopropyl)carbodiimide (EDC), N-Hydroxysuccinimide (NHS).

Other than carbodiimide chemistry, various conjugation chemistry reactions have been employed for chemically introducing the targeting moieties (anti-EpCAM) to the substrate directly or via a linker; for example, imine chemistry, isothiocyanate coupling, diels-Alder reaction, hetero-functional reactions, iminothiolane reaction as depicted in **Figure 7**.[71-74]

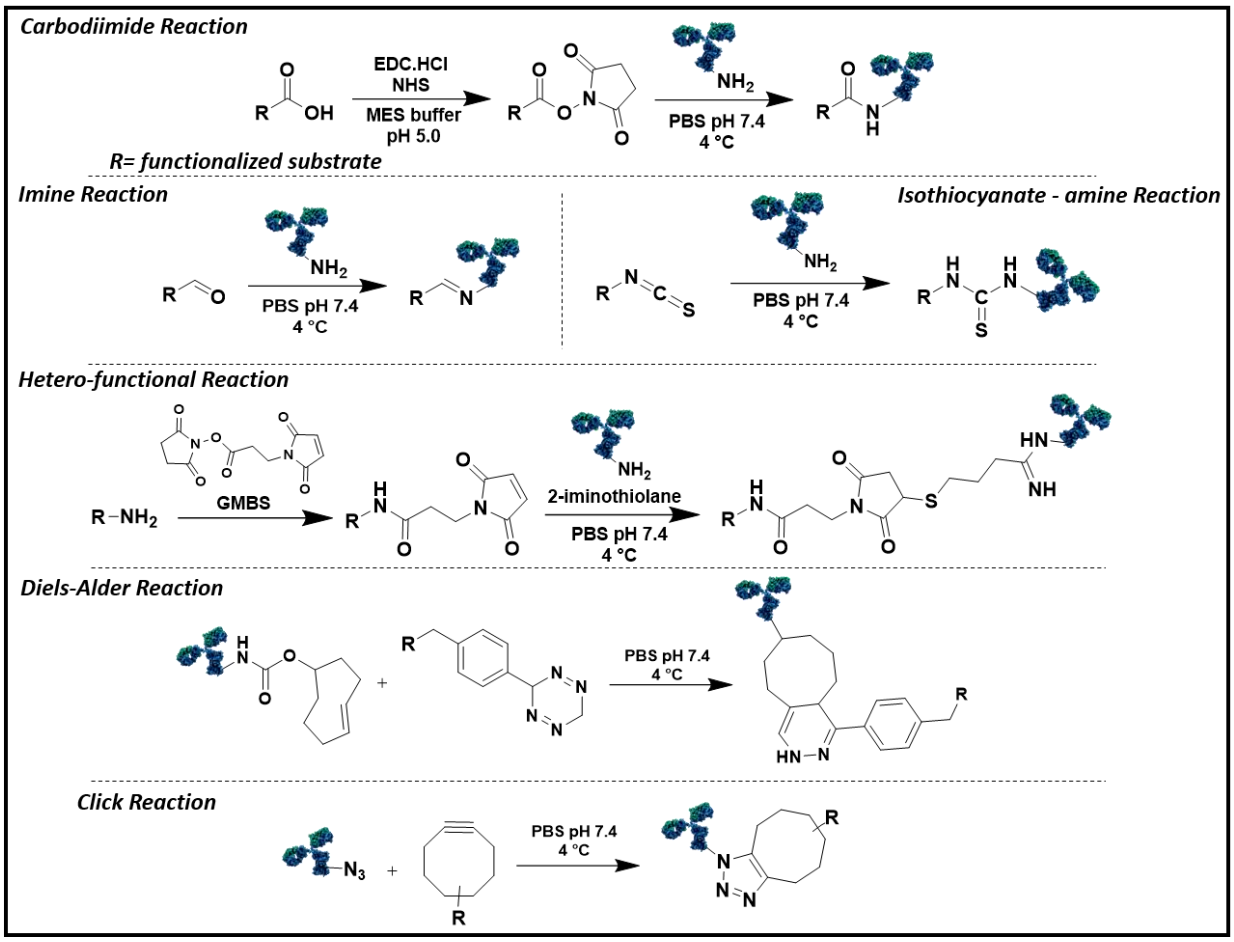

Figure 7: Commonly employed conjugation reactions for coupling nano/micro substrates, possessing different reactive groups with targeting ligands, e.g., transferrin and antibody.

The choice of selecting linkers is even more crucial when conjugating the substates with targeting ligands (anti-EpCAM, aptamer, DNA) as the linker enhances the proximity and probability of antibody-antigen interactions, thereby enabling high CTC capture efficiencies. For example, the long, flexible linker (PEG) or the multivalent, hyperbranched linker (polyamidoamine dendrimer (PAMAM)) allows enhanced local topographic interactions between the nanostructured material and cell surface components (e.g., EpCAM), resulting in a greatly improved cell-capture affinity compared to a short linker.[75-79]

Although capture and isolation of CTCs provide preliminary, diagnostically relevant information, it is conceivable that the CTC-derived molecular signatures and functional read-outs can offer

more valuable and significant insights into tumor biology. This knowledge can produce highly beneficial outcomes if received during the critical window where therapeutic intervention could make a substantial difference. To conduct molecular and functional analyses of CTCs, it becomes crucial to develop materials that can capture CTCs with high efficiency and release CTCs with minimum contamination and negligible disruption to CTC viability and cellular functions.[72, 80-82] In this context, using a stimuli-responsive linker or targeting ligand (DNA, aptamer) enables selective and gentle CTC release from capture substrates upon slight alteration of external conditions, thus enabling downstream CTC *in-vitro* analysis without the use of harsh proteolytic digestion commonly employed to dissociate antibody-antigen interactions.[80] The commonly used stimuli-responsive linkers and their chemical structure have been described in **Figure 8** and discussed in detail in other sections of the review.

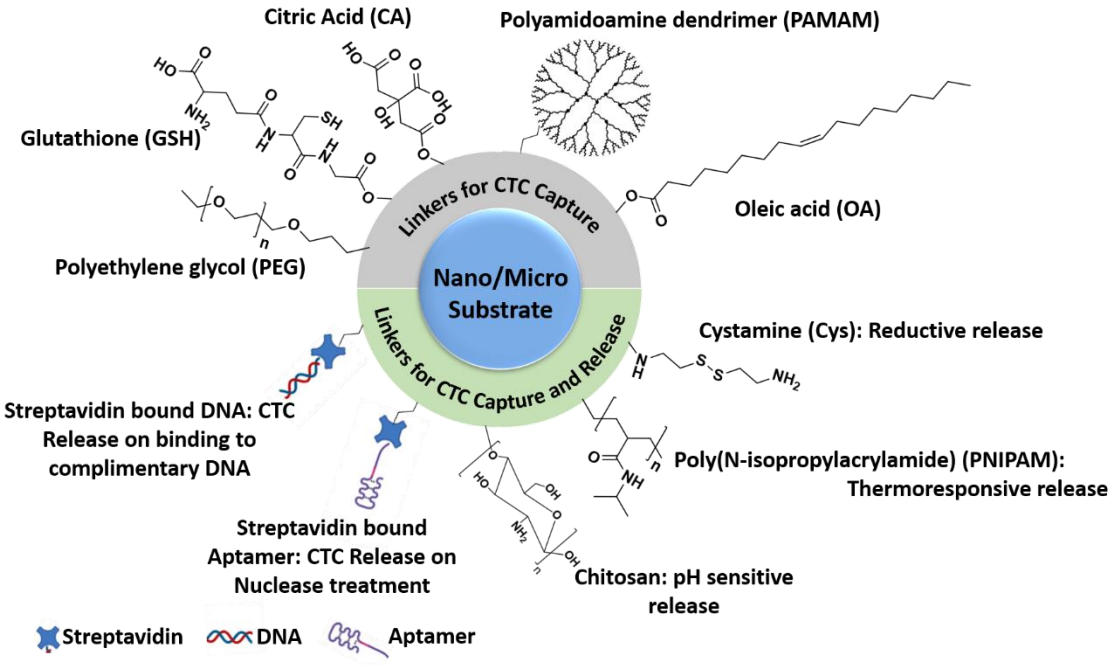

Figure 8: Chemical structures of commonly used reactive linkers for conjugating the nano/micro substrates with ligands to capture CTCs.

Apart from stimuli-responsive linkers targeting ligands, such as aptamers, are also utilized in CTC isolation methodologies, as CTC release post-capture is easily achievable. Aptamers are considered "chemical antibodies," which are short, single-stranded DNA/RNA molecules possessing unique tertiary structures that enable them to bind to target moieties (ions, proteins, small molecules, macromolecules, tissues, cells, etc.) with enhanced affinity and specificity comparable to that of an antibody/antigen interaction.[84,85] In the CTC isolation and analysis field, aptamers have demonstrated increasing potential as alternative recognition ligands to antibodies, which may be scarce due to limited knowledge and availability of target antigenic cancer markers.[85] Consequently, many aptamers against cell-surface expressed cancer biomarkers have been developed, including EpCAM, HER2, EGFR, Mucin 1 (MUC1), Prostate-specific membrane antigen (PSMA), Carcinoembryonic antigen (CEA), etc.[84, 86-89] Furthermore, the ease of labelling and enhanced stability bestow added advantages for the aptamers utility in

microfluidic chip-based systems for CTC isolation.[84] Additionally, the use of aptamers enables the selective and gentle release of CTCs from capture substrates, thus allowing downstream CTC *in-vitro* analysis.[80] In this manner, the release of CTCs would preserve their inherent biological characteristics and greatly facilitate use in downstream applications, thereby enabling further CTC characterization on the cellular, proteomic, and genomic levels.

Tumor over-expressed surface biomarker proteins for targeting CTC isolation

While advanced material interfaces are used to design CTC capture platforms, identifying overexpressed tumor-specific biomarkers is equally essential to ensure specific and efficient capture of CTCs. The tumor biomarkers commonly targeted when developing CTC isolation techniques have briefly been described below.

Epithelial Cell Adhesion Molecule (EpCAM) is a 39-42 kDa glycoprotein, which has been correlated with weaker cell adhesion, contact adhesion, and polarization, suggesting that EpCAM acts as a negative regulator of adhesion; a hallmark of tumor cells.[90, 91] EpCAM was the first clinically validated biomarker shown to be overexpressed in numerous carcinomas and described as "a major epithelial carcinoma antigen."[92] EpCAM tends to be highly overexpressed in multiple epithelial cancers like breast, ovarian, pancreatic, prostate, urothelial, gall bladder, head and neck cancers, etc. and at lower levels in normal epithelial cells.[92-95] High EpCAM expression is often correlated with disease relapse and decreased patient survival.[93-95] Owing to the prevalence of EpCAM overexpression in many carcinomas and CTCs, it has become a "gold-standard" target biomarker in cancer diagnostics, specifically CTC isolation/enrichment technologies.

The tumor biomarker's significance in cancer diagnostics was realized in 2004 when the United States Food and Drug Administration (USFDA) approved the CellSearch® Circulating Tumor Cell Test for use in clinical diagnostic testing for the enumeration of CTCs specifically in metastatic breast, prostate, and colorectal cancers.[96, 97] The immunoassay relies on immunomagnetic materials conjugated to a monoclonal antibody specific to EpCAM, enabling separation of the rare EpCAM overexpressing CTCs from the other blood cells that do not express the tumor biomarker.[98]

Additionally in 2019, the Drug Controller General of India (DCGI) approved the OncoDiscover® Liquid Biopsy Test for clinical cancer diagnostics to detect, capture, and enumerate CTCs in low blood volume (1.5 ml) using an immunomagnetic separation of $EpCAM^+$ tumor cells. Similarly, numerous methodologies to isolate CTCs rely on immunoaffinity-based targeting of this cell surface tumor antigen.

However, it is noteworthy that CTCs in some carcinomas are characterized by variable or negative EpCAM expression patterns ($EpCAM^-$ CTCs).[90, 92, 99] This has been attributed to genotypic and phenotypic changes occurring in CTCs owing to EMT, thereby leading to a downregulation of epithelial phenotype tumor markers (e.g., EpCAM, Cytokeratin, etc.) and upregulation of mesenchymal phenotype tumor markers (e.g., Vimentin, N-Cadherin, fibronectin, etc.).[90, 100] Therefore, methods relying solely on capturing CTCs that are $EpCAM^+$ will not efficiently account for CTCs that undergo EMT, thereby omitting certain subsets of CTCs. Consequently, other tumor markers have emerged as targets for CTC isolation.[90]

Human Epidermal Growth Factor Receptor 2 (HER2; also called Neu/ErbB2), a 185kDA type I transmembrane growth factor receptor protein, is part of the EGFR group of tyrosine kinase receptors.[101] HER2 overexpression is predominantly reported in about 20-30% of human breast and ovarian cancers, generally associated with the more aggressive disease and worse patient outcomes.[101-103] Also, HER2 overexpression has also been documented in Wilm's tumor, bladder cancer, pancreatic cancer, colon tumors, and subsets of gastric, esophageal, endometrial cancers associated with worse disease status; and to a rarer extent in cancers of the oropharynx, lung, and bladder.[102, 103] When taken into consideration, HER2 overexpression across numerous carcinomas has become crucial in validating HER2 targeted CTC isolation strategies. However, like EpCAM-based CTC isolation strategies, the success of HER2-targeted CTC isolation relies solely on the type of carcinoma under-diagnosis and whether HER2 overexpression is a hallmark feature of that particular cancer.

Folic Acid Receptor: Folate deficiency is associated with numerous diseases, including cancers (e.g., breast, ovarian, colon, etc.). Folate receptors are cysteine-rich cell-surface glycoproteins that strongly bind folic acid (FA).[104] These receptors exist in three isoforms: FRα, FRβ, and FRγ. Of the three isoforms, FRα is the most widely studied. While FRα exhibits restricted expression in normal cells, it is highly expressed in various non-mucinous epithelial tumors.[105] It is known that over 95% of ovarian cancer (OC) patients overexpress FRα, where the concentration of FR increases in concentration with tumor progression and is associated with decreased survival.[104] Consequently, there is considerable interest in targeting FRα receptor overexpression on the CTC surface for their isolation; specifically, in OC and other non-mucinous epithelial tumors.

Transferrin Receptor: Transferrin (Tf) is an 80kDa glycoprotein and is part of a family of iron-binding blood plasma glycoproteins that binds ferrous iron (Fe^{3+}) and prevents it from travelling throughout the body in this form, which is toxic to cells, thereby transporting and delivering iron into cells by interactions with its TfR.[106] Significantly upregulated expression of TfR is observed on cancer cells as compared to their normal counterparts.[106] This increased TfR expression is generally correlated with advanced tumor stage and poorer patient prognosis.[106] Consequently, these observations have validated the use of Tf as a ligand model for the capture of TfR^+ CTCs.[107] Therefore, numerous research groups have reported the use of Tf-conjugated substrates for CTC enrichment in both cancer cell lines and different cancer subtypes, including breast cancer, HNC, colon cancer, etc.[107-111]

Before clinical validations, the chemical-based CTC targeting substrates conjugated to tumor-specific targeting ligands are generally validated in cancer cell lines expressing tumor-specific biomarker proteins to test for specificity and efficiency of CTC enrichment. For example, the commonly used tumor cell lines overexpressing cell surface EpCAM protein are MCF-7, HCT 116, A549, Hep G2, etc. Additional examples of cancer cell lines and their overexpressing cancer biomarkers, along with their relevant targeting ligands, have been detailed in **Table 1**.

Table 1: Commonly used cancer cell lines utilized in CTC enrichment-based studies.

Cancer Cell lines	Cell Type	Overexpressed Cancer Biomarker	Capture Antibody/Ligand	References
MCF-7	Human breast ductal carcinoma	EpCAM	Anti-EpCAM antibody	[112-116]
A549	Human lung carcinoma	EpCAM	Anti-EpCAM antibody	[115, 117-119]
Panc-1	Human pancreatic ductal carcinoma	EpCAM	Anti-EpCAM antibody	[78]
Hep G2	Human hepatocellular carcinoma	EpCAM	Anti-EpCAM antibody	
HCT116	Human colorectal carcinoma	EpCAM Tf-receptor	Anti-EpCAM antibody Transferrin	[109, 117]
A431	Human epidermoid carcinoma	EpCAM EGFR	Anti EpCAM antibody Anti-EGFR antibody	[81, 117]
SkBr-3	Human breast adenocarcinoma	HER2	Anti-HER2 antibody	[113, 117, 120, 121]
HeLa	Human cervical adenocarcinoma	Folate receptor	Folic acid	[118]

A schematic representation of different targeting ligands conjugated to a CTC capturing substrates via a chemical linker and their interaction with specific tumor overexpressed cell surface receptors present on CTC is represented in **Figure 9**. Generally, targeting ligands recognize molecular shapes and complementary sequences on cell surface receptors, and the better the fit in terms of geometry, the higher the affinity between them, ultimately leading to stronger interactions. These interactions between cell surface receptors and targeting ligand exclusively involve non-covalent bonds in a similar manner as enzymes bind to their substrates. These interactions are reversible and easily dissociated by high ionic strength or under extreme pH conditions.

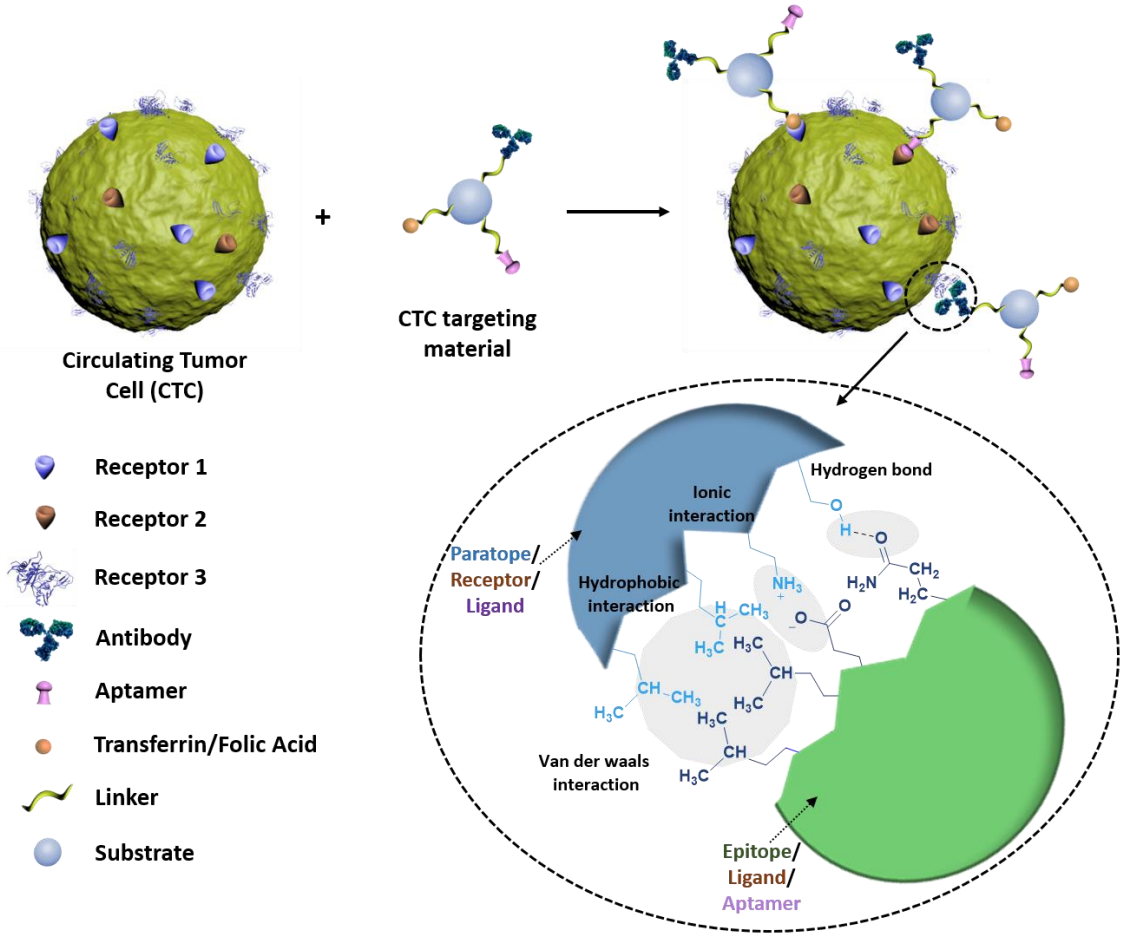

Figure 9: Schematics representing non-covalent interactions between CTC surface biomarker proteins and the biomarker targeting ligands conjugated to the nano and micro substrates. Information adapted from ref.[122]

2. Chemo-specific multi-component nanomaterials for CTC enrichment

Designing multi-component nanomaterials can effectively improve the sensitivity and efficiency of CTC capture enrichment and detection. Moreover, as discussed earlier, the inimitable properties of nanomaterials, as discussed earlier, can overcome the limitations of CTC detection. This section will focus on the material design interface with respect to magnetic nanomaterials, which are the gold standard in CTC isolation.[123]

Functionalizing iron oxide magnetic nanoparticles for CTC capture.

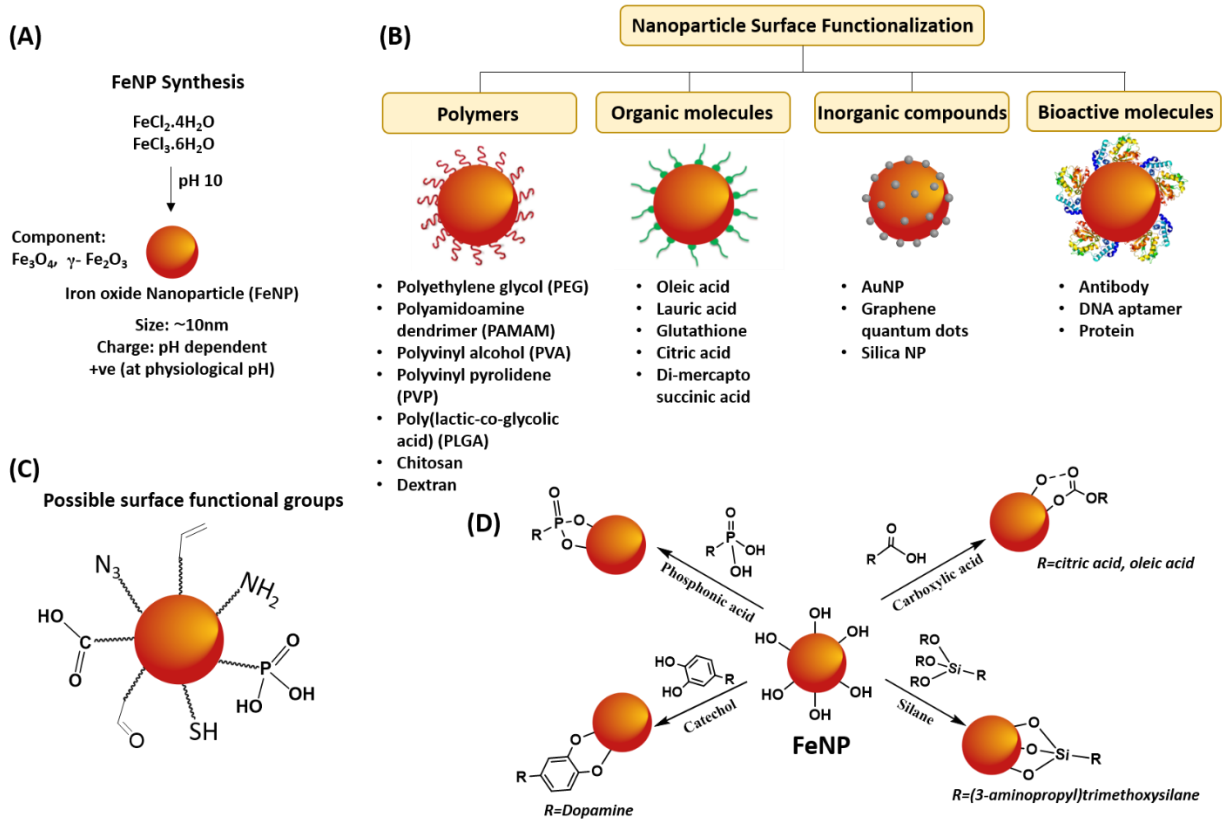

Figure 10: Schematics for surface functionalization of FeNP. **A)** Preparation by co-precipitation method; **B)** Coating and surface functionalization; **C)** Possible reactive groups; **D)** Schematic illustration showing the introduction of organic functionalities on FeNP.

The variety of applications engaging FeNP, such as labelling and magnetic separation of biological materials, MRI contrast enhancement, directed drug delivery, hyperthermia treatment, has brought about a tremendous increase in designing their synthetic methodologies. The most relevant synthetic approaches include co-precipitation, thermal decomposition, sonolysis, sol-gel processes, spray and laser pyrolysis, hydrothermal and high-temperature synthesis, nanoreactors, and microwave-assisted synthesis.[124-141] Thus, to have the desired control over the physicochemical properties of nanoparticles such as size, shape, charge, stability, dispersibility, etc., it becomes highly essential to choose the synthetic methodology carefully.

Based on the size, magnetic particles are ordered as large (1.5 to about 50 μm), small (0.7-1.5 μm), or colloidal (<200nm), similarly denoted to as nanoparticles.[142] As noted, magnetic enrichment is the preferred method for cell separations, and the nanoparticles employed for this purpose do not have to be removed before cell analysis. Accordingly, the nanoparticles should be small enough to not interfere with analytical measurements, i.e., below 200 nm. Furthermore, the nanoparticle should be large enough and magnetically responsive to permit cell separation using an external magnetic field. Additionally, the uncoated colloidal magnetic particles possess a sufficiently high positive charge at physiological pH (**Figure 10**). Therefore, the coating material should preferably be applied to prevent nonspecific interaction between the magnetic core and biological macromolecules, such as sialic acid residues on the non-target cell surface, lectins,

glycoproteins, and other cell membrane components. Several base coating materials have been described in the literature, such as polymers, organic molecules, inorganic materials, and biomolecules. However, lately, the attention is shifted to molecules that can provide an additional and high-density iron nanoparticle functionalization to further the conjugation reaction (**Figure 10**).

Iron oxide nanoparticle-based enrichment methods are among the first and most widely used techniques to isolate, enumerate, and detect relevant tumor biomarkers such as CTCs *in vitro* from whole blood samples.[143] Immunomagnetic separation technique is advantageous due to exclusive magnetic property including, easy handling with a magnet, possible surface coating, chemical coordination of reactive groups on FeNPs and further linking with bio-functional ligands of interest, higher surface-volume ratio, sufficient dispersibility in biological medium and relatively acceptable bio-compatibility.[96, 144, 145] The immuno-magnetic affinity system involves FeNPs conjugated to targeting moieties, that evidence non-covalent interactions with CTCs and thus enable their separation via an external magnetic field.[97] In short, magnetic nanoparticles have been the most crucial platform in CTC enrichment techniques, and maximum CTC detection research is focused on using magnetic nanoparticles. Even the commercialized technologies approved by regulatory bodies for CTC enrichment and detection utilize magnetic nanoparticles linked with anti-EpCAM antibodies, two of which are described below.

CellSearch® Circulating Tumor Cells Test. The CellSearch® system uses bovine serum albumin (BSA) coated magnetic nanoparticles of size 90-150 nm. The BSA coated nanoparticles were then coupled to streptavidin with sulfosuccinimidyl 4-(N-maleimidomethyl)cyclohexane-1-carboxylate using heterobifunctional chemistry. For antibody coupling, monobiotinylated antibody was reacted with streptavidin magnetic nanoparticles for 1 hour. The remaining active streptavidin sites were blocked with biotinylated-BSA (**Figure 11**).[96, 97] The use of multilayer protein (BSA, streptavidin) on nanoparticles reduces nonspecific interaction with other blood components compared to uncoated nanoparticles, and utilization of monoclonal antibody (anti-EpCAM) shows high specificity for a particular EpCAM epitope. The enrichment method comprises of mixing blood samples of the cancer patient with colloidal magnetic beads coupled to antibody targeting the tumor-associated antigen (EpCAM) on the CTC surface,[146,] but which does not enrich other cellular and non-cellular components of the blood above a baseline threshold of EpCAM expression. Subsequently, the blood-magnetic particle mixture is subjected to a magnetic field to produce a cell fraction enriched in antibody-coupled magnetic particles bound CTCs. Finally, the enriched fraction of CTCs is analyzed. The tumor cells present in the sample can be characterized by cellular and molecular markers to determine prognostic and predictive disease status. This system utilizes automated digital microscopy to identify and enumerate CTCs and is proved to have a sensitivity of 87.7%. The CellSearch system has been widely accepted in clinical utility, however, with few limitations, i) the detection cost is very high as CellSearch uses biotinylated monoclonal antibodies, ii) the CTCs cannot be isolated for heterogenicity phenotype identification and molecular analysis since the system captures $EpCAM^{+}$ cells, iii) the sensitivity and selectivity are comparatively low.[147]

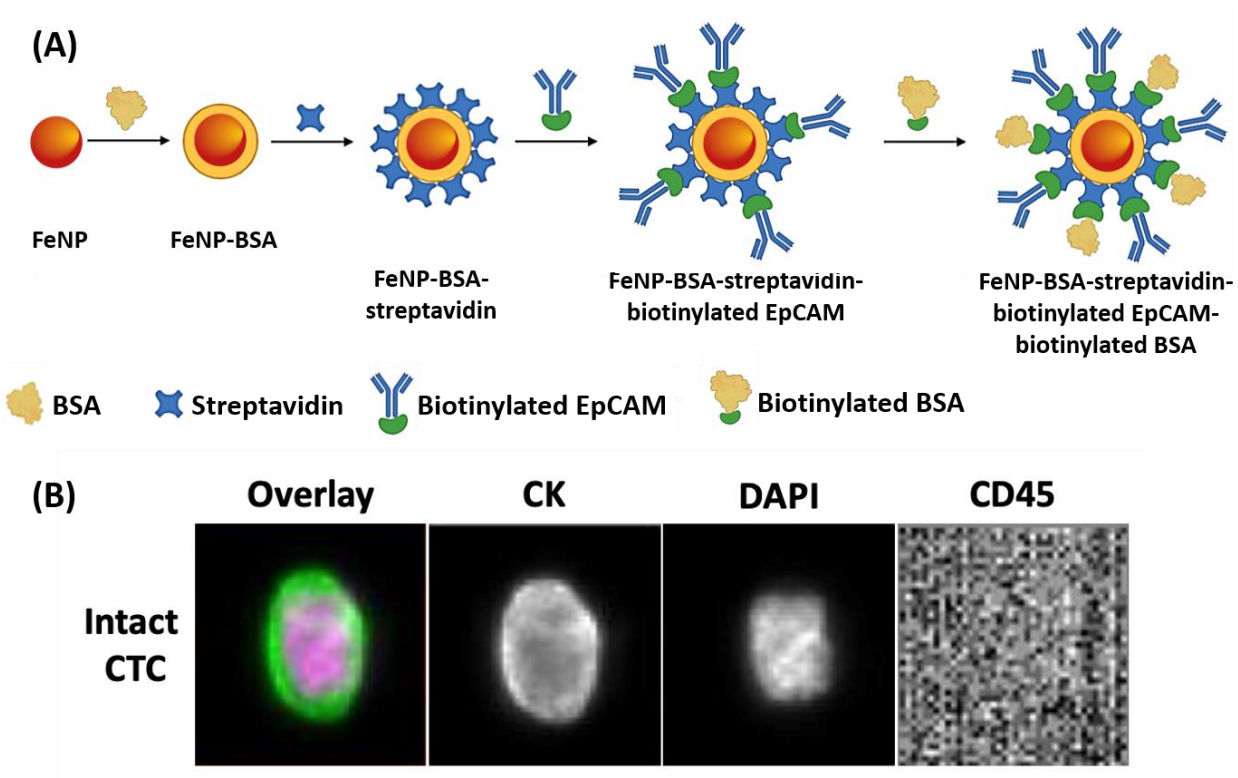

Figure 11: **A)** Schematics representing surface functionalization of FeNP with targeting ligands utilized in the CellSearch® Circulating Tumor Cell Test; **B)** Representative image of intact CTC isolated from NSCLC patient blood using CellSearch® Circulating Tumor Cell Test. CTC is positive for CK staining as well as nuclear stain DAPI but negative for leukocyte antigen CD45. Adapted from ref.[148]

OncoDiscover Liquid Biopsy Test. Recently, an immunomagnetic affinity-based CTC diagnostic test was approved by the Central Drugs Standard Control Organization (CDSCO, India) for detecting epithelial cancer cells from bladder, prostate, neuroendocrine, liver, pancreatic, lung, breast, head and neck, colorectal, ovarian, and stomach.[33, 34, 37, 145] The OncoDiscover Test, based on the OncoViu® platform, uses a multi-component system consisting of glutathione-linked iron nanoparticles covalently conjugated to carbon allotropes like CNT and graphene via PAMAM dendrimer as a linker. Finally, the iron NP-CNT substrate is decorated with optimized amount of EpCAM antibodies via carbodiimide chemistry (**Figure 12**). The multi-component system provides a high density of functional groups for anti-EpCAM immobilization, thus, increasing the availability of cell recognition sites resulting in enhanced cell capture efficiency. The OncoDiscover test immunomagnetically enriches cells overexpressing EpCAM. The captured cells expressing Cytokeratin 18 are characterized by the immunofluorescence (IF) method using a combination of fluorescent dyes (anti-cytokeratin and anti-CD45). The in-vitro diagnostics test can rapidly isolate, detect, and enumerate CTCs with high precision, specificity, and efficiency. However, like CellSearch®, there exists the potential to miss subpopulations of CTCs expressing non-epithelial phenotypes or that have undergone EMT with dramatically decreased EpCAM expression.[149]

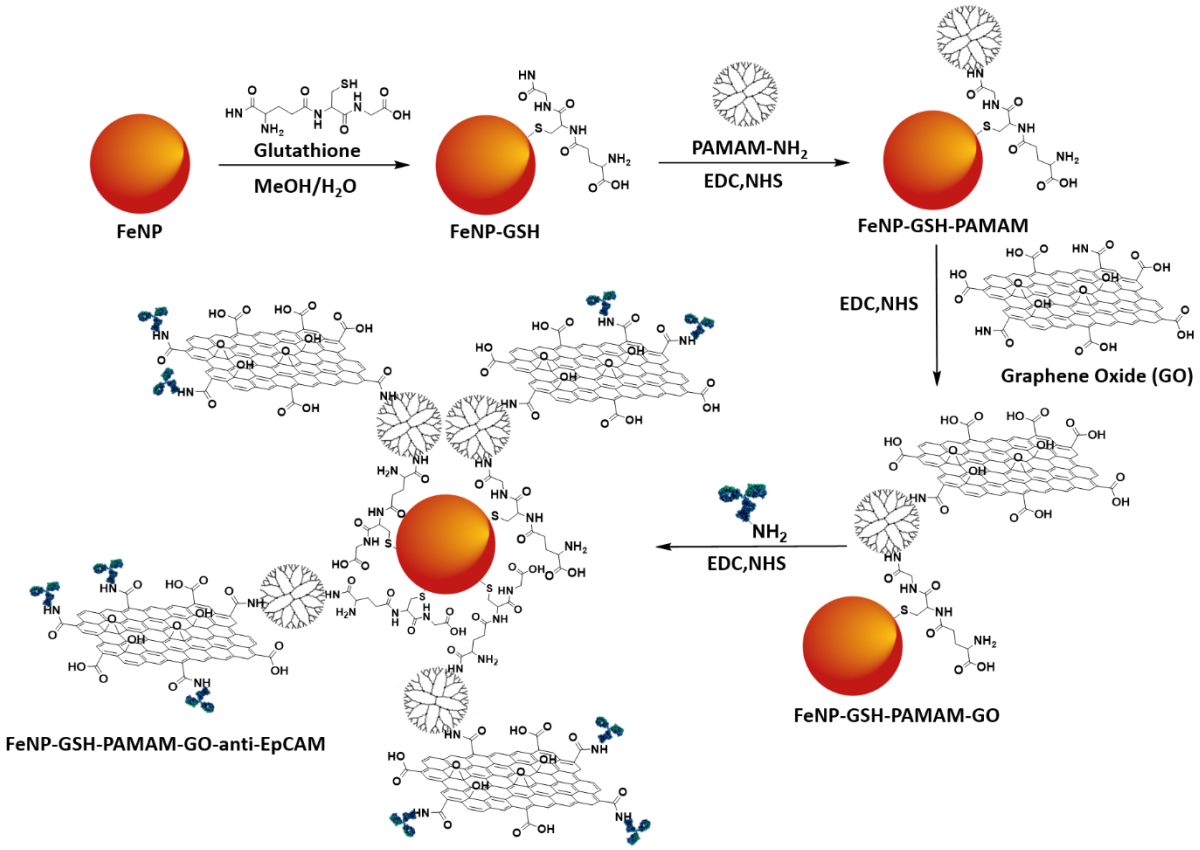

Figure 12: Preparation of multi-component material for isolation of CTCs using OncoDiscover. Multivalent linker (PAMAM), graphene oxide (GO) sheets, anti-EpCAM have been conjugated onto glutathione coated FeNP using carbodiimide coupling reactions.

These commercial technologies have been engineered on the advances made in recent years in the field of material designs. Racila et al. reported the first use of magnetic NPs for enrichment, detection, and characterization of carcinoma cells in the blood.[143] Since then, much advancement has been substantiated in the material interface to decrease the nonspecific interaction to increase the bio-specificity toward targeting marker. For example, Ding e al. established a method for efficient capture and sensitive fluorescent labeling of CTCs based on near-infrared fluorescence Ag_2S (silver sulphide) nanodot-based signal amplification combined with immunomagnetic spheres.[112] The design consisted of the conjugation of anti-EpCAM onto the surface of oleic acid stabilized magnetic nanoparticles via carbodiimide coupling. Oleic acid prevents the iron nanoparticles from agglomeration and protects them from unwanted interaction with blood samples. In addition, these magnetic nanospheres labeled anti-EpCAM antibodies showed high capture efficiency (>95%) of CTCs, with a lower limit of 6 CTCs, in MCF-7 cells spiked blood samples.

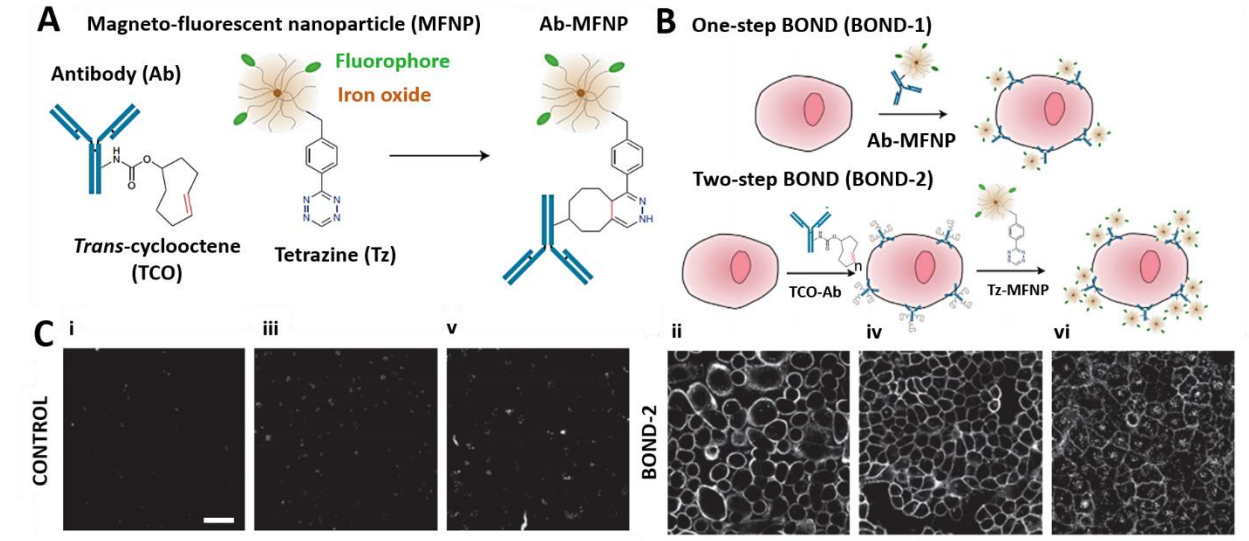

Figure 13: **A)** Bioorthogonal reaction between 1,2,4,5-tetrazine labelled fluorescent magnetic nanoparticles and trans-cyclooctene labelled antibody; **B)** Use of BOND for one-step and two-step targeting of NPs to cells; **C)** Confocal microscopy images of labelled live cells. Control: non-binding, TCO-modified control antibody (clone MOPC-21). HER2 (i,ii); EpCAM (iii,iv); EGFR (v,vi). Scale bar: 50mm. Figure adapted from ref. [117]

In an exciting publication, Haun et al. delineated a bio-orthogonal nanoparticle detection (BOND) method, demonstrating the employment of the Diels-Alder reaction for CTC enrichment.[117] The process employed a simple, rapid, and catalyst-free cycloaddition Diels-Alder reaction interfacing tetrazine (Tz) and transcyclooctene (TCO). The authors used a BOND chemistry-based system for labelling carcinoma cells using a two-step approach: antibodies against biomarkers of interest (EpCAM, HER2, EGFR) were modified with transcyclooctene and incubated with cell lines (HER2 for SK-BR-3, EpCAM for HCT 116 colon cancer cells, and EGFR for A549 lung cancer cells). Then, transcyclooctene modified cells were then directly resuspended with tetrazine modified magnetic nanoparticles (MNPs) to the couple via cycloaddition reaction (**Figure 13**). Since multiple tags could modify one antibody without the loss of affinity, multiple attachments of Tz-MNPs to cells were subsequently achieved using the antibodies as scaffolds. Therefore, parallel to the cell-MNPs preparation method directly using MNP-antibody conjugates, the two-step BOND strategy was efficiently amplified by MNP-binding to cells leading to enhanced efficiency and detection sensitivity. The material was validated with different antibodies (Anti-HER2, anti-EpCAM, anti-EGFR antibody) against various cell lines (HCT 116, SK-BR-3, A549, NCI-H1650, A431, etc.).

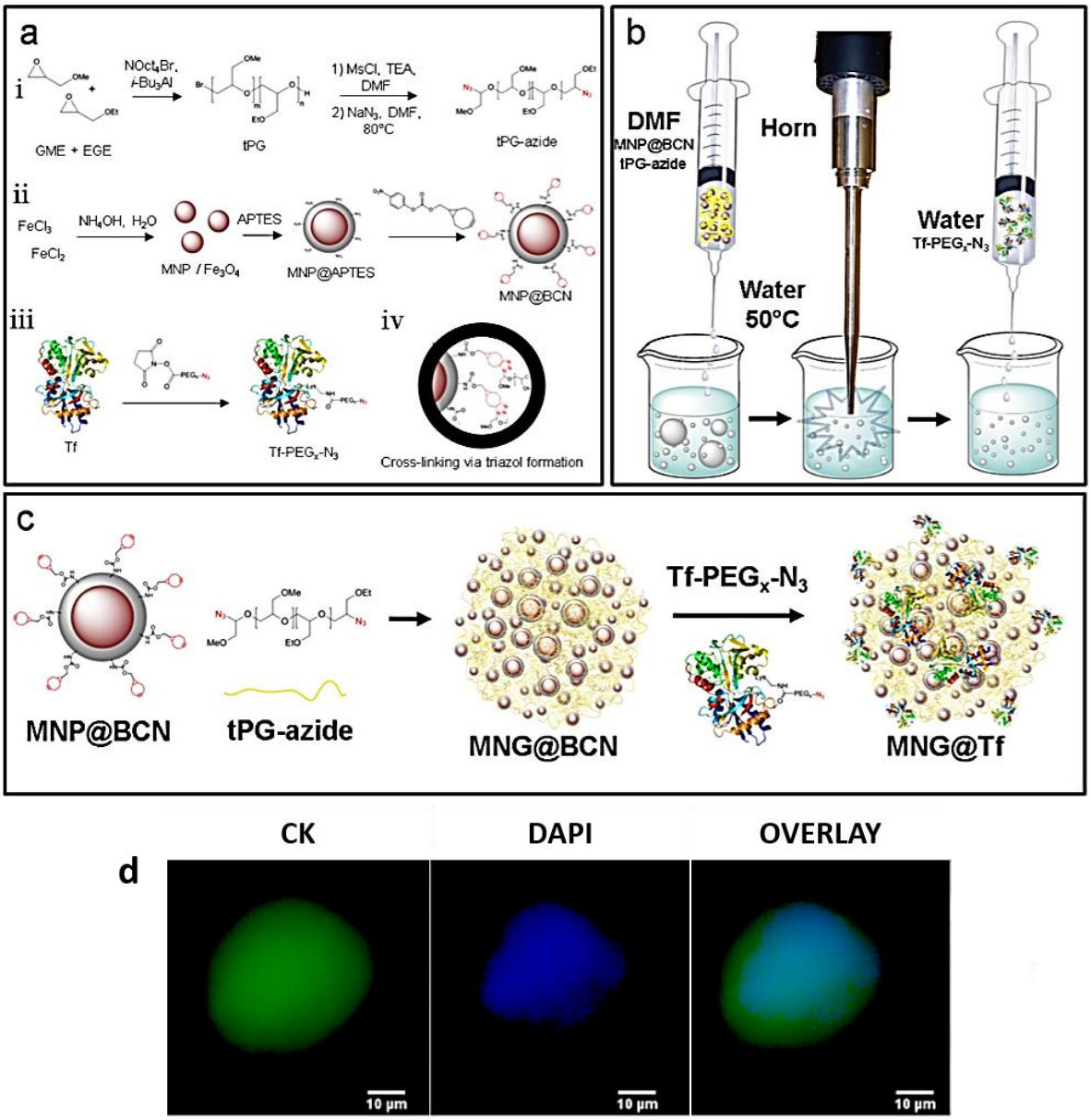

Figure 14: Magnetic nanogels with multiple ligands for enhanced CTC isolation. **a)** Synthesis of nanogel precursors, namely (i) linear thermoresponsive polyglycerol (tPG) with azide functionalities via polymerization of glycidyl methyl ether (GME) and ethyl glycidyl ether (EGE), (ii) magnetic nanoparticles decorated with bicyclononyne (MNP@BCN), and (iii) Tf-functionalized PEG-N_3. **b-c)** A typical procedure for the synthesis of magnetic nanogels via ultrasound-assisted thermo-nanoprecipitation. **d)** Representative fluorescence image of CTC captured using magnetic nanogels from breast cancer patient's blood. Captured CTC is CK (green) and DAPI (blue) positive. Figure adapted from ref.[107, 150]

Magnetic polymeric nanogel system with multiple ligands for CTC capture.

Crosslinked polymer networks, especially those with three-dimensional nanogels as substrate, protect the magnetic core from nonspecific interactions with blood components and provide

surface functionality for biomolecules conjugation. Moreover, nanogels using hyperbranched polymer chains may offer unique rheological traits due to multiple reactive functional groups. In addition, phase separation of such systems induced due to physicochemical stimuli such as temperature and pH results in selective biological interactions.

For example, Calderon et al. designed magnetic nanogels (MNGs) consisting of iron oxide NPs that selectively captured CTCs from a breast cancer patient's blood sample.[107, 151] MNGs were yielded following ultrasound-assisted thermo-nanoprecipitation via alkyne-azide strain-promoted click chemistry, as previously developed by the same group.[151] Iron oxide NPs were decorated with bicyclononyne (MNP@BCN) and used as crosslinkers and anchoring points for post-synthetic PEGylation (**Figure 14**). Glycidyl methyl ether (GME) and ethyl glycidyl ether (EGE) were polymerized in a ring-opening polymerization process to yield thermoresponsive polymers suitable for MNGs preparation. The surface of MNGs was decorated with Tf using PEG of varying lengths to target the overexpressed Tf receptors on CTCs. The material was optimized with respect to (a) linker/spacer between the magnetic core and Tf, (b) density of linkers coupled to the MNGs, and (c) molecular weight of the thermoresponsive polymer. Comparison between PEG with various (4,8,12 units) ethylene glycol (EG) units revealed 8 units EG as the optimal linker length with the highest CTC capturing efficiencies. Moreover, the spacer to transferrin ratio also had a key role with optimal value at three linkers per Tf, attaining 81% CTC capturing efficiency with Tf^+ HCT116 cell lines.

Capture and release of CTCs using nano-magnetic substrates.

The significance of CTC release post-capture for the downstream analysis has been explained in previous sections. Lu et al. described well-established interaction, streptavidin-biotin system, decomposable immunomagnetic iron oxide beads for CTC capture and released.[81, 152] To evidence this, a short peptide sequence, Trp-Ser-His-Pro-Gln-Phe-Glu-Lys, Strep-tag II, was conjugated with an anti-EpCAM antibody, which was specifically interacted with Strep-Tactin coated magnetic beads (STMBs) to obtain antibody-modified STMBs. The design was finally evaluated for capturing $EpCAM^+$ A431 human epidermoid carcinoma cell lines (**Figure 15**). After the magnetic separation of A431 cells, the STMB was treated with biotin. Since strep-tactin has a stronger affinity for biotin, it forces Strep-tag II derived antibody to detach from STMBs, enabling the release of A431 cells. Additionally, anti-EpCAM functionalized STMBs were used to isolate and detect CTCs in cancer patients' peripheral blood samples. The method showed 79% capture efficiency, and 70% of the CTCs isolated were released by the addition of biotin, and about 85% of the released cells remained viable. Similar chemistry was published by Bai et al. wherein EpCAM recognition peptide Pep10 (VRRDAPRFSMQGLDACGGNNCNN) was conjugated onto MNPs (~200 nm) via biotin-avidin interaction. The material successfully captured and enriched human breast cancer MCF-7 and SK-BR-3 cells, prostate cancer PC3 cells, liver cancer Hep G2 cells for rare cell and demonstrated comparable efficiency (>90%) and purity (>93%) with anti-EpCAM coated MNPs for breast, prostate and liver cancers from spiked human blood under magnetic field.[113]

Zhou et al. proposed using multifunctional magnetic luminescent nanoparticles (MLNPs) for fast, efficient, cell-friendly capture and recovery of CTCs.[114] The material composition comprised of the quantum dots (QDs) (CdSSe/ZnS) that were deposited on poly(allylamine hydrochloride) coated magnet-responsive (Fe_3O_4-PAH) nanoparticles. Subsequently, PAH and hyaluronic acid

(HA) layers were deposited through a facile layer by layer assembly method. The desired MLNPs (PAH/QD/PAH/HA) were successfully built to monitor the capture and recovery process in real-time. The surface carboxylic groups of MLNPs were functionalized with cystamine dihydrochloride 50% molar ratio (cys: carboxyl group), and the remaining carboxylic groups were PEGylated via carbodiimide chemistry. The obtained nanoparticles were treated with dithiothreitol (DTT) to cleave the cystamine disulfide bonds, and subsequently, the thiolated nanoparticles were reacted with N-succinimidyl-3-(2-pyridyldithio)propionate (SPDP) to generate free terminal NHS ester. Finally, the nanoparticles were decorated with an anti-EpCAM antibody. The exquisiteness of these MLNPs is that in the existence of glutathione (GSH), the disulfide bond between cys-SPDP would cleave, thereby releasing the captured CTCs. The MLNPs showed 99% capture efficiency using MCF-7 cell lines ($EpCAM^{+}$). Moreover, on GSH treatment, cell viability was investigated using the Live/Dead staining method, displaying almost 100% cell release efficiency with 98% cell viability.

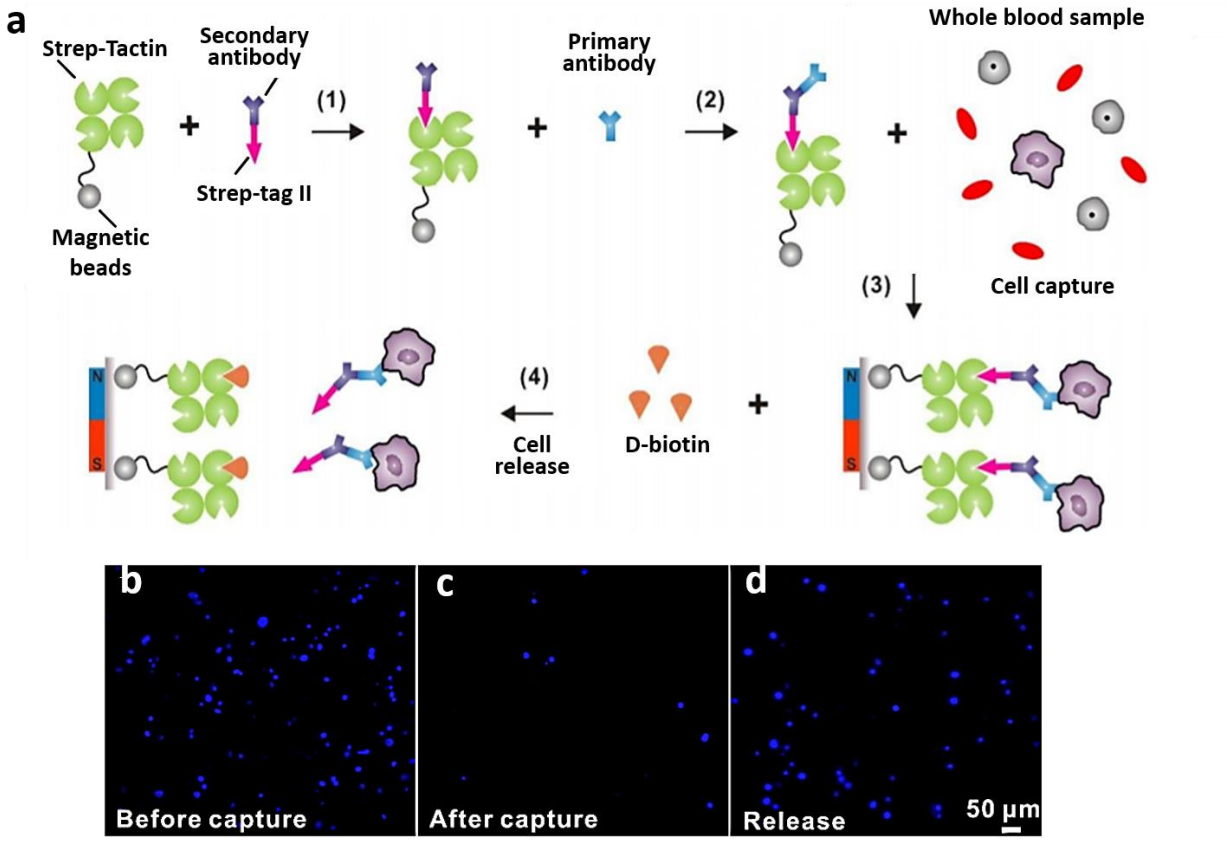

Figure 15: Schematics for immunomagnetic based CTC enrichment methods. **a)** Strep-Tactin coated magnetic beads (STMBs) for CTC capture and their biotin triggered release (1) Strep-tag II labeled Secondary Antibody (anti-mouse IgG) reacted with STMBs; (2) Anti-EpCAM, anti-EGFR or anti-HER2 interacted with IgG-STMBs for grafting antibody over IgG-STMBs; (3) Antibody grafted STMBs used to capture CTCs; (4) Biotin triggered the release of captured CTCs; Capture and release of cancer cells **(b-c)** Fluorescent microscopic images of SK-BR-3 cells before (b), after (c)

incubation with anti-EpCAM-IgG-STMBs; Released SK-BR-3 cells **(d)**. Reprinted with permission from ref. [81]

Xiao et al. utilized the principle advantage of deoxyribonucleic acid (DNA) aptamer and their easy cleavage by introducing a DNA complementary sequence or nuclease, to capture and release CTCs (**Figure 16**).[115] DNA aptamer, a single-stranded nucleic acid molecule that binds targets of interest in an antibody-like manner, possesses several advantages over antibodies, such as shorter generation time, lower manufacturing costs, consistency between batches, higher modifiability, enhanced thermal stability, and enhanced target potential from ions to live animals.[154] The synthetic methodology of the reported material involved the preparation of polyethyleneimine (PEI)-stabilized iron nanoparticles (Fe_3O_4@PEI NPs) that were dip-coated with PEI/polyvinyl alcohol nanofibers via a blended electrospinning process to obtain magnetic short nanofibers (MSNFs). Further, these composite nanofibers (Fe_3O_4@PEI/PVA) were crosslinked with glutaraldehyde vapors for improved stability in water. Amine-functionalized MSNFs surface was then modified with 3-(maleimido)propionic acid N-hydroxysuccinimide ester. Finally, surface conjugation of DNA aptamer was performed through thiol-maleimide coupling to generate aptamer-MSNFs. The developed aptamer-MSNFs specifically captured MCF-7 ($EpCAM^+$) cancer cells with 87% efficiency and enabled the non-destructive release of cancer cells with 91% release efficiency after nuclease treatment.[80] Even though, aptamer-MSNFs exhibited high capture efficiencies (83-94%) for various $EpCAM^+$ cancer cells (MCF-7, 88%; A549, 94%; and HepG2, 83%), the capture efficiency for $EpCAM^-$ cancer cells (HeLa) was quite low i.e. around 3.2%.

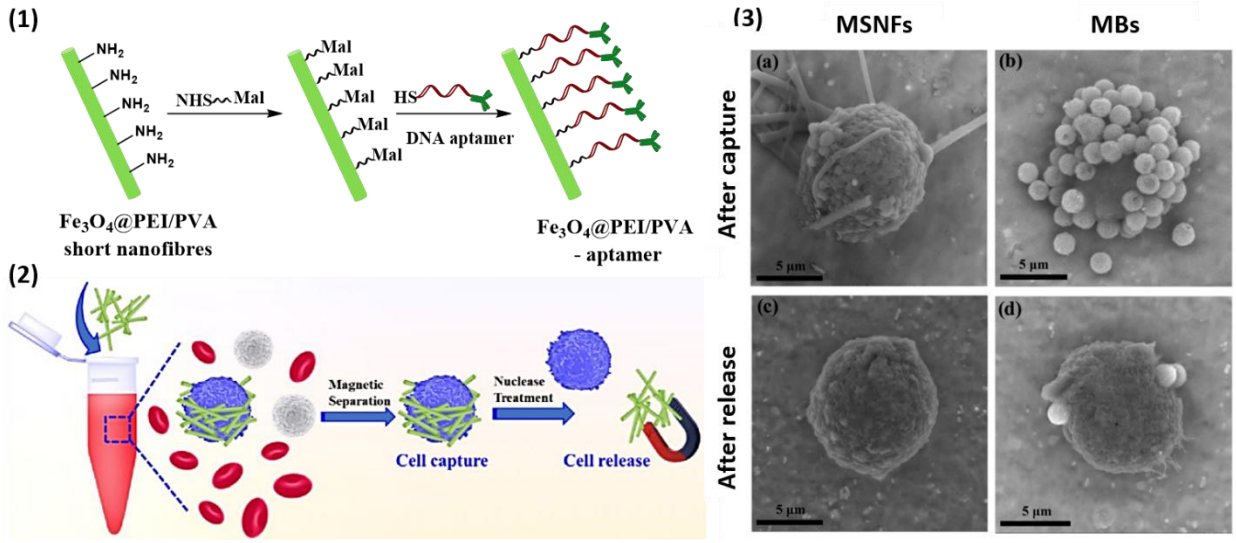

Figure 16: **(1-2)** Schematic depiction of the surface modification of MSNFs for cancer cell (MCF-7) capture and release applications; **(3)** SEM images of MCF-7 cells after capture by (a) aptamer–MSNFs and (b) aptamer–Magnetic beads and after release treatment (c) to remove the MSNFs and (d) to remove the MBs.[115]

Micro-rockets with a propellent motion for CTC interaction and capture

Iron oxide-based CTC capture platforms have shown great promises in isolation and enrichment of CTCs from peripheral blood. Interestingly, the employment of another nanostructure system

combined with iron oxide nanoparticles, such as FeNP-Graphene or FeNP-CNT can further enhance the material's efficiency, selectivity, and specificity. Such a system would help provide synergistic augmented multivalences and a high density of functionalization units per molecules for efficient ligand-receptor interactions. For example, a graphene/CNT oxide - Iron oxide NPs, is a synergistic system wherein graphene/CNT offers a higher number of functionality (free acidic group) per molecule for antibody conjugation and iron nanoparticles core can be magnetically separated from the bulk.

In this context, Banerjee et al. described a multi-component material involving H_2O_2-driven O_2 bubble-propelled micro rockets to precisely capture CTCs.[109] The micro rocket system consisted of three functional components: (i) CNTs for increasing surface area, (ii) magnetic NPs for isolation, and (iii) transferrin for specific CTC targeting. The chemical mechanism in the form of oxidation using CNTs was introduced to generate carboxylic acid functionality, followed by the loading of iron oxide NPs within the inner surface of CNTs by incubating oxidized CNTs with divalent and trivalent iron chloride salts. Finally, transferrin was functionalized on the CNT-Fe_3O_4 via carbodiimide chemistry (**Figure 17**). The self-propulsion of suspended Tf-CNT-Fe_3O_4 microparticles mimicked a micro rocket due to the oxidative release of O_2 in the existence of H_2O_2, with the speed of the micro rocket being dependent on the percentage of H_2O_2 concentration. This self-powered system allowed ~85% efficiency (TfR^+) to capture human colorectal carcinoma (HCT) 116 cells and CTC extraction from biological fluids.

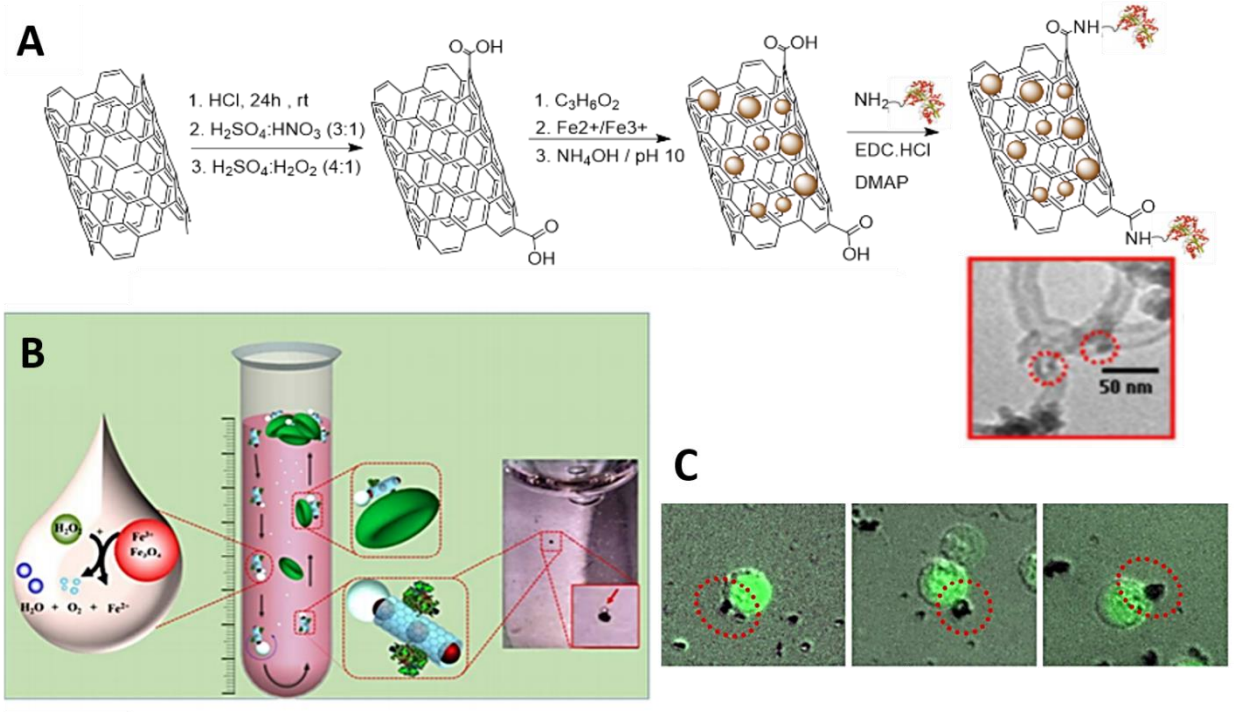

Figure 17: A) Tf-CNT-Fe_3O_4. Inset shows a TEM image of Tf-Fe_3O_4-CNT. (red dotted circles indicate presence of Fe_3O_4 in CNT); **B)** Schematic of the driving mechanism for the Tf-Fe_3O_4-CNT micro rocket. The right side inset shows the upward moving Tf-Fe_3O_4-CNT micro rocket due to the

oxidative release of O_2 in the existence of H_2O_2, as indicated by an arrow; **C)** Fluorescence image of Tf-CNT-Fe_3O_4 micro rocket attached to the HCT116 cells in just 5 min. Adapted from ref.[109]

Conversely, Li et al. designed magnetic halloysite nanotubes (MHNTs) - folic acid composite to target the Folic acid (FA) receptor on cancer cells.[118] The MHNTs composite was synthesized by mixing HNTs with trivalent iron and divalent iron salts using a one-step co-precipitation method. Next, these MHNTs were functionalized with Ad-PEG-FA (Admantane-PEG-Folic acid), using carboxylated β-cyclodextrin (CD) as a linker, to get MHNTs@β-CD@Ad-PEG-FA. The material's specificity was determined by incubating MHNTs@β-CD@Ad-PEG-FA nanocomposite with 100,000 Skov3, Hela, or A549 cells. The peak efficiency of 95.6% (for all cell lines) was obtained compared to non-FA receptor normal HEK 293T, which showed <10% efficiency.
Recently, Quadir et al. stated water-dispersible 'nanocages' composed of cellulose nanocrystals (CNCs), covalently linked to magnetic FeNPs (**Figure 18**).[110] These systems were composed of cellulose nanocrystals (CNCs) obtained from biobased resources. Multiple hydroxyl groups on CNCs render the molecule ideal for the multivalent conjugation of CTC-targeting ligand (Tf). [155] In addition, these functional groups also provide a hydrophilic microenvironment for the captured CTCs. The native CNCs were functionalized using epichlorohydrin chemistry to generate multiple amine functional groups. Through iminothiolane-mediated immobilization of thiol groups on these amines, these authors were able to conjugate FeNPs, and succinylated transferrin. While the metal-thiol interaction was characterized by X-ray photoelectron microscopy and high-resolution TEM, the success of covalent conjugation of Tf-succinate to amine-functionalized CNC was followed by IR spectroscopy. The synthesized product was found to organize in the form of a metal 'nanocage' where the metal NPs were found to be stabilized within the CNC cross-linked matrix. The authors also observed that such a self-organized structure was magnetically active and formed stable nanoscale colloids with an average particle size of 254.0 ± 6.0 nm. The presence of NPs ensured that the nanocages were magnetic and thus enabled CTC capture. Tf-CNC-based nanocages were compared with clinically relevant OncoViu platform for the CTC capturing efficiency using the blood samples of HNC patients. It was observed that the efficiency of CTC isolation using CNC-derived nanocages, was about 85% compared to the OncoViu platform.

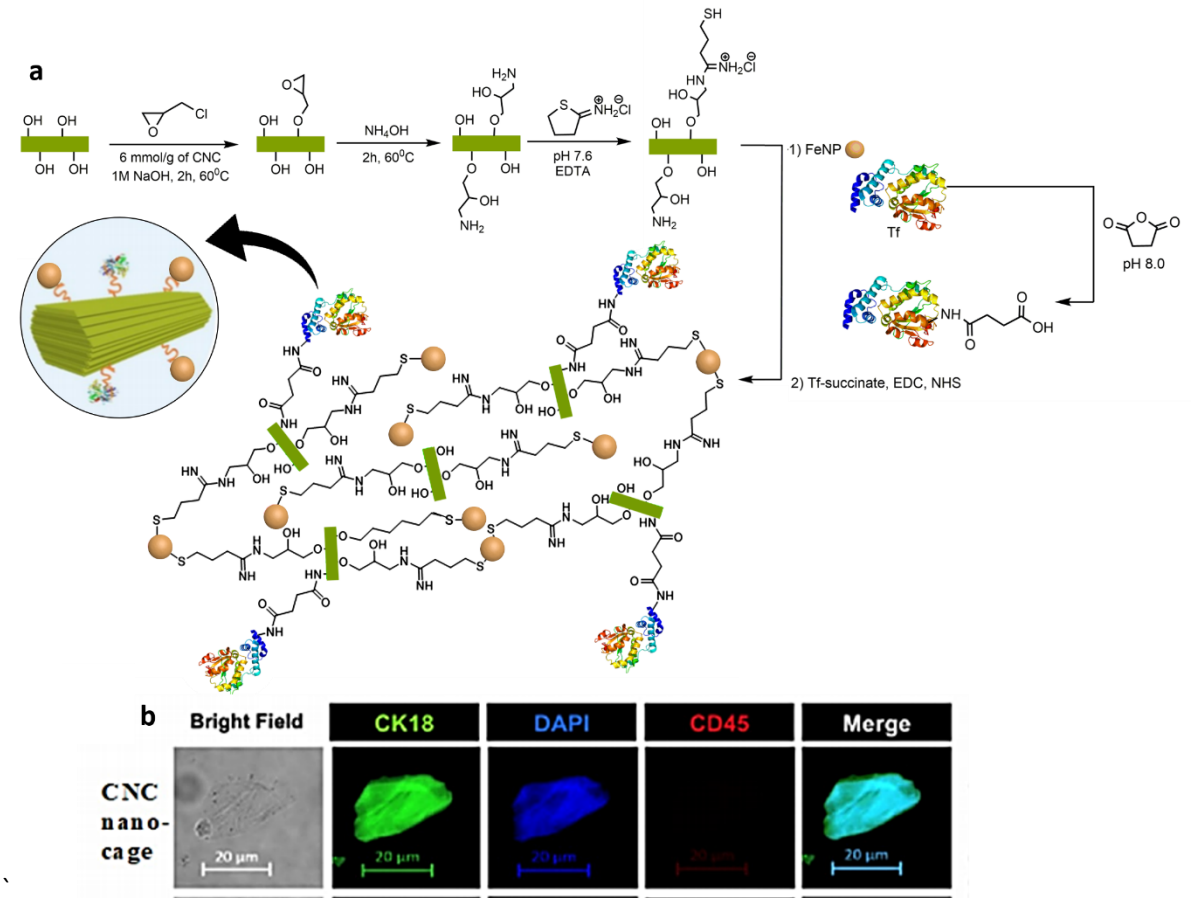

Figure 18: **a)** Synthetic scheme for conjugation of cellulose nanocages to iron nanoparticles followed by functionalization with transferrin; **b)** Fluorescence image of isolated CTCs by CNC nanocages from a blood sample of HNC patient. Captured cells were labeled with CK18 (green), CD45 (red), and DAPI (blue): nuclei staining. Figure adapted from ref.[110]

Shi et al. published another chemo-specific design having multiple discrete components, including multi-functional graphene oxide quantum dots (GOQDs) and magnetic nanoplatform for selective separation and diagnosis of hepatocellular carcinoma (HCC) tumor CTCs from infected blood.[156] The multi-component nanosystem offered paramagnetism and multiphoton luminescence that allowed magnetic separation of enriched CTC followed by two-photon imaging. The system comprised of GOQDs conjugated to MNPs via amine-modified PEG using carbodiimide coupling. Finally, monoclonal anti-GPC3 antibody grafted over GOQDs using EDC, NHS chemistry. Here PEG serves not only as a linker for localized spatial movement of the antibody but also prevents nonspecific interactions with blood cells. Antibody decorated GOQDs-MNPs displayed 97% capture efficiency while only GOQDs-MNPs showed only <2% efficiency.

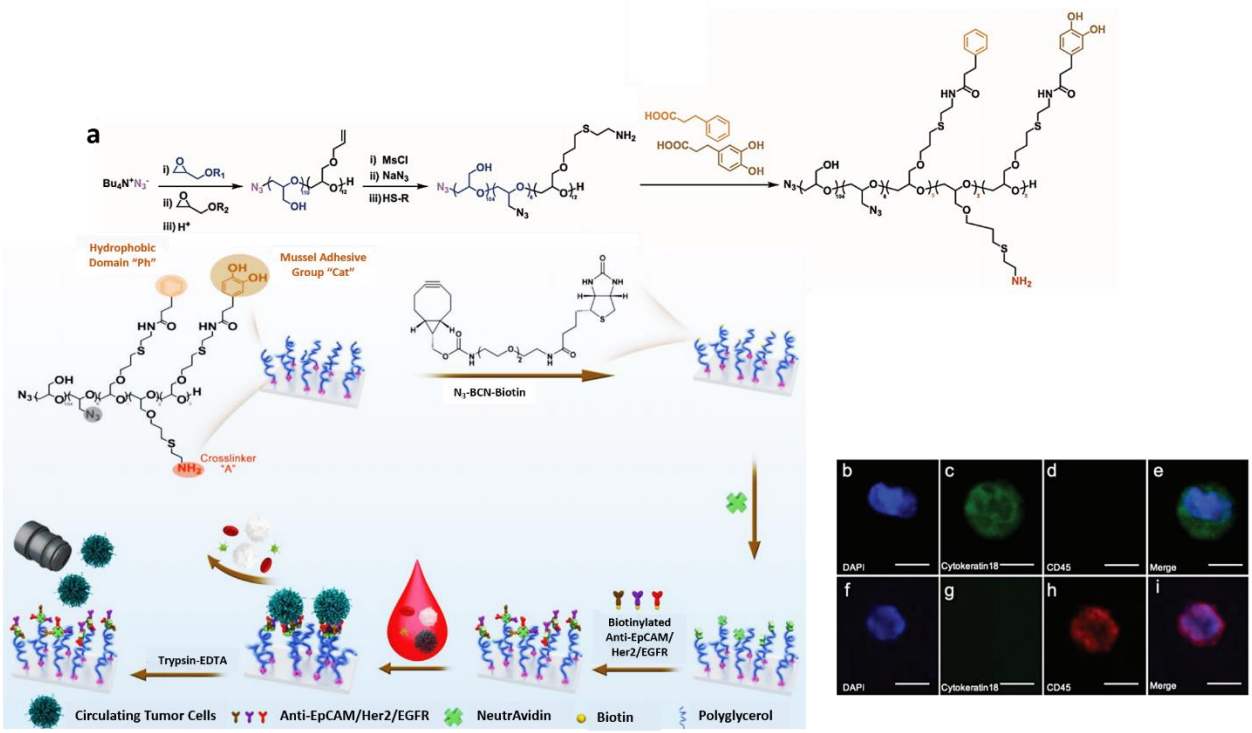

Figure 19: Schematic illustration for the preparation of polyglycerol based copolymer used for coating TiO_2 functionalized glass surface. **a)** Synthesis of polyglycerol based coating copolymer with cathecol and phenyl groups as an anchoring agent, which mimics mussel adhesion. While the terminal azides serve as post functionalized sites; **b-i)** Fluorescence image of isolated CTCs and WBCs on the substrate, stained with DAPI (blue), anti-cytokeratin18 conjugated with Alexa Flour 488 (green), and anti-CD45 conjugated with Alexa Flour 532 (red) respectively from advanced breast cancer patients. Scale bar indicates 5 µm. Figure adapted from ref.[119]

Glass surface coating for multivalent CTC capture with high sensitivity.

Haag et al. established a polyglycerol-based block polymer functionalized glass surface as a bio-specific interface for CTC isolation with higher selectivity.[119] Titanium dioxide (TiO_2) slides were prepared via chemical vapor deposition (CVD) of TiO_2 onto clean glass cover slides.[157] Titanium dioxide slides were then functionalized with polyglycerol (PEG) based poly(ethoxyethyl glycidyl ether)-block-poly (allyl glycidyl ether) (PEEGE-b-PAGE) copolymer with catechol groups and phenyl groups as the anchoring agent, which mimicked mussel adhesion (**Figure 19**). The terminal and side-chain azide (N_3) groups were coupled to the cyclooctene groups of BCN-biotin via catalyst-free azide-alkyne cycloaddition reaction. The slides were then functionalized with streptavidin and finally with biotinylated anti-EpCAM/Her2/EGFR. The clinical utility of functional surface coating was tested by capturing CTCs from the advanced breast cancer at stage II and III patients' blood. High CTC count ranging from 49 to 217 CTCs mL^{-1} (mean = 112.2 CTCs mL^{-1}) were obtained in the advanced breast cancer patients. For low EpCAM expressing cell lines, i.e., the MDA-MB-231 cell and A549 cell, multivalent antibodies (anti-EpCAM, anti-Her2, and anti-EGFR) were integrated into the surface coating to obtain an improved efficiency of > 90%.

3. Chemo-specific multi-component microfluidic system for CTC Enrichment (Flow-through System)

As noted above, CTC capture platforms delineated with iron oxide nanoparticles have shown good CTC capturing efficiency (80-100%), but their utility is limited to a small volume of blood (1 to 10 mL). Moreover, the amount of antibody-conjugated iron oxide nanoparticles used per milliliter of blood is very high, and the detection process requires a complicated enrichment step. Therefore, lately, the microfluidic platform has emerged extensively for CTCs' detection and isolation. They possess several advantages over conventional methods such as automatic operation, range of sample volumes (10^{-9} mL to 10^{2} mL), reduced target cell loss, high sensitivity, and throughput. Moreover, it functions as a one-step process for sample collection, loading, isolation, and analysis, resulting in significantly reduced processing time and avoids loss of rare CTCs for multiple experimental steps. Various materials such as glass, ceramics, metals, and polymers have been utilized to fabricate fluidic platforms. Among all the candidates, glass and polydimethylsiloxane (PDMS) are the most used owing to their chemical flexibility, rapid prototyping, gas permeability, optical properties, cost efficiency, and biological compatibility. Furthermore, the fluidic platform can be easily functionalized with a very low volume of reagent/targeting ligand (such as an antibody) using simple coupling reactions that can be integrated with other nanomaterials/nanotechnologies for improving capture efficiency. In the past decades, researchers have studied microfluidic-based CTC enrichment techniques by utilizing the unique properties of CTCs such as density, size, deformability, surface protein expression, etc.[158-161] However, below, we review the advances in chemistry employed in flow-through devices to enrich CTCs based on their surface biomarker expression.

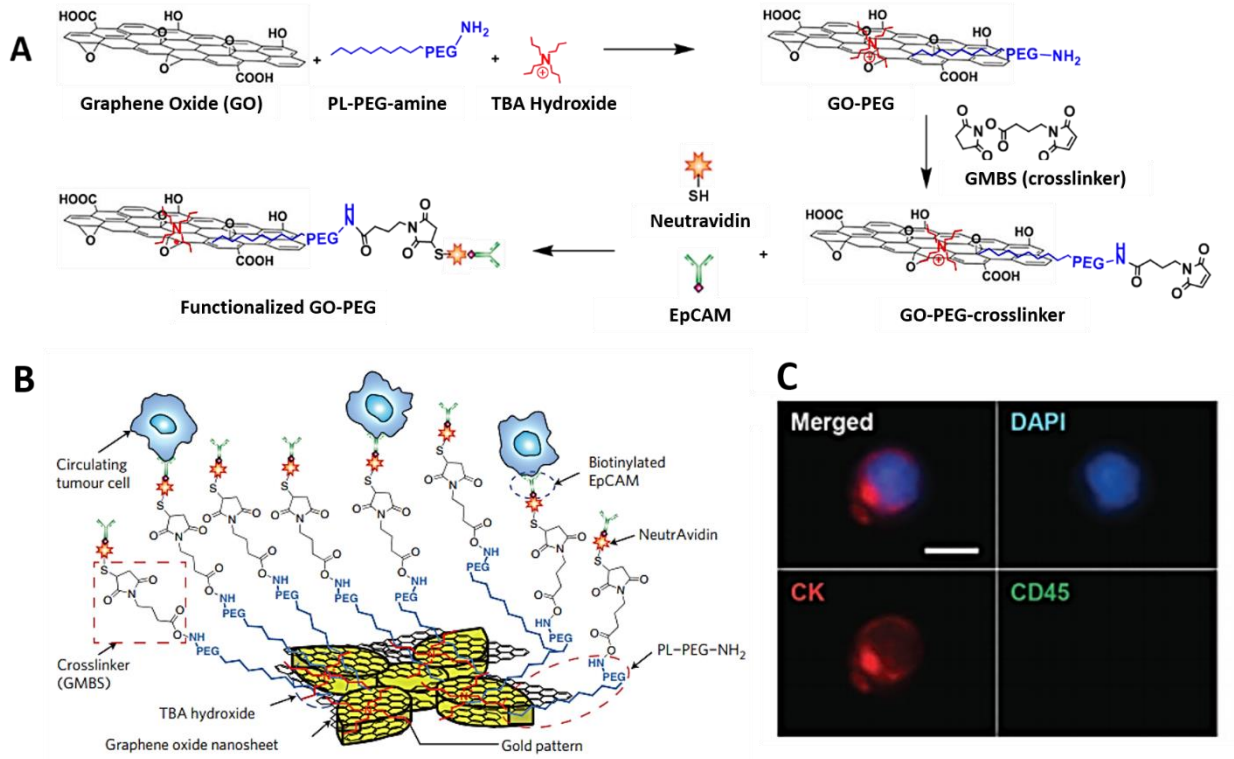

Figure 20: **A)** Synthetic Protocol for functionalizing GO-PEG on the PDMS layer conjugated to the biotinylated antibody via Neutravidin; **B)** Schematic of device functionalization with GO chips

fixed onto a gold patterned surface; **C)** Representative image of isolated CTC stained for $DAPI^+/CK^+/CD45^-$, showing individual and merged fluorescence channels. Adapted from ref.[162]

A fluidic methodology consisting of graphene oxide (GO) nanosheets patterned over PDMS fluidic channels was adapted by Kim et al. to isolate CTCs from metastatic breast cancer patients.[163] The chip fabrication consisted of a silicon substrate with a flower-shaped gold pattern. The device's overall size was 24.5 mm × 60 mm × 3 mm, and the height of the PDMS microfluidic chamber was 50 µm. Firstly, phospholipid-polyethylene-glycoamine (PL-PEG-NH_2) was non-covalently immobilized on GO nanosheets. Tetrabutylammonium (TBA) hydroxide was used for achieving complete exfoliation and intercalation of the GO. Following, GO nanosheets were adsorbed onto the decorated gold surface in a microfluidic chamber. The amino group of PL–PEG–NH_2 on GO sheets coordinated with the patterned gold surface by electrostatic attraction.[164] Additionally, N-γ-maleimidobutyryloxysuccinimide ester (GMBS) was introduced, having N-hydroxysuccinimide (NHS) esters, which further was used for reacting with the amine groups of PL–PEG–NH_2 on the GO, forming amide bonds. Next, thiolated NeutrAvidin was introduced in the chamber coupled to the maleimido group of GMBS on the GO sheet. Finally, biotinylated anti-EpCAM was coupled to NeutrAvidin via NeutrAvidin-biotin interaction (**Figure 20**). Incorporating GO as the substrate of the antibody conjugation chemistry allowed CTC detection from 1 mL of blood with high efficiency due to the presence of dense antibody. The unique design allowed blood processing at a flow rate of 1 mL h^{-1} while offering surface capture of CTCs with extremely low blood cell contamination, which is essential for multiple downstream analyses at both proteomic and transcriptional levels.

The short survival and rarity of tumor cells in blood require appropriately sensitive and specific techniques to identify CTCs from among billions of other blood cells. The choice of bioconjugation method and antibody linking is critical to ensure adequate cell capture but are often poorly understood mechanisms. In a report, Andree et al. demonstrated the binding affinity constants of the EpCAM antibodies EpAb3-5, MJ-37, VU1D-9, and HO-3 by Surface Plasmon Resonance imaging (SPRi).[120] They reported a fluidic glass assembly by adhering two antibody-coated microscopic glass slides together. Glass surface was first functionalized with a monolayer of 3-aminopropyl(triethoxy)silane (APTES). APTES functionalized glass slides were then placed in a slide holder and treated with a poly(acrylic acid) (PAA), EDC, and NHS to obtain the NHS-activated PAA layer. Finally, the epitope of EpCAM antibodies EpAb3-5, VU1D-9, MJ-37, and HO-3, were treated with the NHS activated glass surface. Next, SPRi was performed to compare the binding affinity of the 4 different epitopes of EpCAM antibodies. Highest binding affinity was showed by EpAb3-5 ($K_D = 2.6E^{-11}$ M) comparable to the affinity of HO-3 (KD = $4.0E^{-11}$ M) followed by VU1D-9 (KD = $2.7E^{-10}$ M) and MJ-37 respectively (KD = $2.8E^{-9}$ M). The capture efficiency of these epitopes of EpCAM antibodies was determined against breast carcinoma cell line SKBR-3 ($EpCAM^+$) and the capture efficiency correlated with the K_D values, i.e., more cells captured by antibodies with higher K_D values. These results emphasize that thorough tests should be performed to make the best choice for the desired application when choosing an antibody for such applications.

Moreover, regardless of antibody selection, the design of antibody interfacial molecular organization is pivotal in determining the capture performance. The molecules/spacer, which binds the surface of the microfluidic device to biomolecule (e.g., EpCAM antibody), plays a fundamental role in the efficiency of the microfluidic device. Unlike nanostructures, the

antibodies are not dispersed in a microfluidic device but are rather fixed to the device's surface. Therefore, a longer, flexible spacer allows the movement of antibodies in the small vicinity to efficiently capture CTCs compared to a small spacer, which keeps the antibodies fixed at one place without any movement.

Yeh et al. correlated the importance of linker/spacer on a substrate with CTC isolation efficiency.[78] Conventionally, the antibody molecules were conjugated on the surfaces of microfluidics. Consequently, the total number of antibodies−antigen pairs may be limited by the fixed number of antibody molecules per surface area underneath a cell. Polymer brushes or dendrimers as the long flexible linkers may sidestep the shortcomings of short-chain linkers by promoting local, short-range antibody−antigen clustering.[79]

The same group developed three different microfluidic devices where the first device antibodies were coated via a fixed linker resulting in restricted accessibility to each cell antigen. In the second device, antibodies were coated via lipid molecules in a supported lipid bilayer (SLB) with 2-dimensional lateral mobility, resulting in antibody-antigen clustering on the SLB plane. Finally, in the last device, antibodies were coated via long spacer arm dendrimer-SLB, allowing both lateral and vertical mobility for entropic favored spatial arrangement, resulting in maximal antibody-antigen pair formation.[78] Incorporating the stretchable PAMAM dendrimer proved to be an excellent mediator facilitating a multivalent effect due to their capability to pre-organize/orient ligands and easily deformable polymeric chains to allow easy antibody-antigen interaction. The introduction of dendrimer (flexible linker) and a laterally mobile lipid bilayer circumvent the shortcomings of short-chain linkers by promoting local, short-range antibody−antigen clustering. Compared to capture by surface lipid bilayer microfluidics only, over 170% enhancement in capture efficiency for Panc-1 cells (even for low EpCAM expressing cells) was observed using PEG-PAMAM-SLB system.

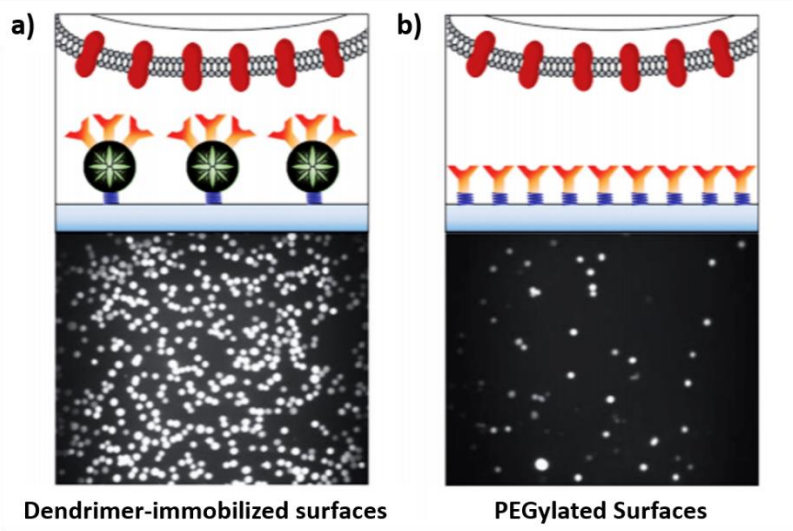

Figure 21: Schematic illustration for CTC capture on dendrimer- and PEG- immobilized surfaces. Cell adhesion experiments using **(a)** dendrimer immobilized surfaces showed significant enhancement in CTC capture compared to **(b)** PEG immobilized surfaces. Captured tumor cells were visualized using surface plasmon resonance. Adapted from ref.[79]

Similar enhanced binding avidity through a multivalent binding effect using dendrimer was demonstrated by Myung and coworkers, which significantly improved the selectivity for CTC detection.[79] The cell capture efficiency on the surfaces functionalized with anti-EpCAM dendrimer (PAMAM) / linear polymer (PEG) conjugates were tested on three cancer cell lines (MDA-MB-361, MCF-7, MDA-MB-231) under static and dynamic conditions (**Figure 21**). Under static conditions, a significantly high number of cancer cells were bound on the dendrimer coated surface (up to 15.2-fold) compared to the PEG-coated surface. High capture efficiency was maintained underflow on the dendrimer coated surface (up to 3.7-fold) compared to the PEG-coated surface.

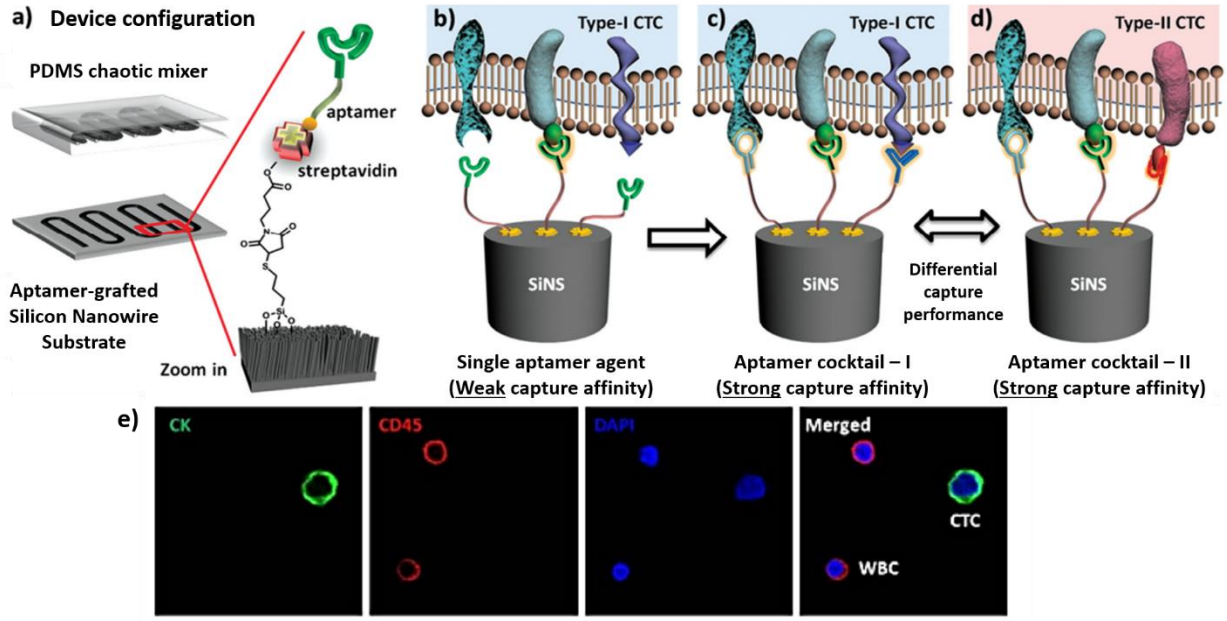

Figure 22: Aptamer cocktail CTC capture. **a)** Microfluidic CTC chip composed of aptamer grafted SiNWs laid on PDMS mixer; **b)** Single aptamer capture agent showing lack of synergistic binding; **c)** Cocktail capture agent showing synergistic binding leading to an enhanced capture affinity; **d)** Different cocktails of capturing agents for CTC subpopulation interactions; **e)** Fluorescence image of captured CTC and WBCs from non-small cell lung cancer patient. Adapted from ref. [165]

Liquid biopsy, the enrichment of CTCs shed from solid tumors, and their enumeration through minimally invasive approach provided an opportunity to address a long-standing oncology challenge, the real-time monitoring of tumor status, and analysis of tumor heterogeneity. However, even after years of effort, specific and efficient isolation, capture, and detection of CTCs with diverse phenotypes are still perplexing. To enable the comprehensive characterization of CTC heterogeneity, it is crucial to improve enrichment processes that meet the demand of sufficient capture specificity, efficiency, and the capability to isolate cancer cells with different phenotypes.

Zhao et al., while addressing the issues of tumor heterogeneity and limited availability of antibodies against tumor-specific surface markers, developed a microfluidic system using the aptamer cocktails synergistic effect.[165] The microfluidic chips were composed of two separate components, a patterned silica nanosubstrate (SiNS) and a PDMS (polydimethylsiloxane) chaotic

mixer.[167] The SiNS was first silanized with (3-mercaptopropyl)trimethoxysilane followed by conjugation with N-γ-maleimidobutyryloxysuccinimide ester (GMBS). Subsequently, streptavidin was grafted over SiNS followed by functionalization with four different biotinylated aptamers (Ap1, Ap2, Ap3, and Ap4). These aptamers target other surface markers on CTCs. Aptamer cocktails with a synergistic effect showed a better overall CTC capture efficiency than a single aptamer against NSCLC cell lines and NSCLC patients' blood samples (**Figure 22**). Head on comparison of anti-EpCAM and aptamers, and the aptamers showed almost 300% more efficiency than anti-EpCAM.

As noted microfluidic system shows greater promises for CTC isolation and enrichment, but the only major limitation of microfluidics is the reduction of capture efficiency with increasing blood flow as the fluid flow rate defines the duration of cell-antibody (protein) interaction.[168] Therefore, it becomes essential to maintain a low shear force in the capillary flow channel platform to maximize the attachment of CTCs, which in turn consumes time. This limits the efficiency of CTC isolation from large blood volumes.

Capture and Release of CTCs using a flow-through system.

Shen et al. developed a nanoVelcro fluidic chip consisting of biotinylated aptamer grafted on the silicon nanowires (SiNWs) via streptavidin-biotin interaction.[80] The NanoVelcro chip showed >90% efficiency with NSCLC CTCs. A next-generation NanoVelco chip was reported by the same group consisting of silica nanowires (SiNWs) covalently grafted with thermoresponsive polymer poly(N-isopropylacrylamide) (PNIPAM) and biotinlyated anti-EpCAM decorated over the nanostructure via streptavidin-biotin chemistry (**Figure 23**).[169] The nanostructure was capable of capturing NSCLC CTCs with high efficiency and additionally could release the immobilized CTCs upon a change in temperature as an external stimulus. Interestingly, there was an insignificant difference in CTC capture efficiency between PNIPAM grafted anti-EpCAM-SiNWs and anti-EpCAM-SiNWs.[80, 169]

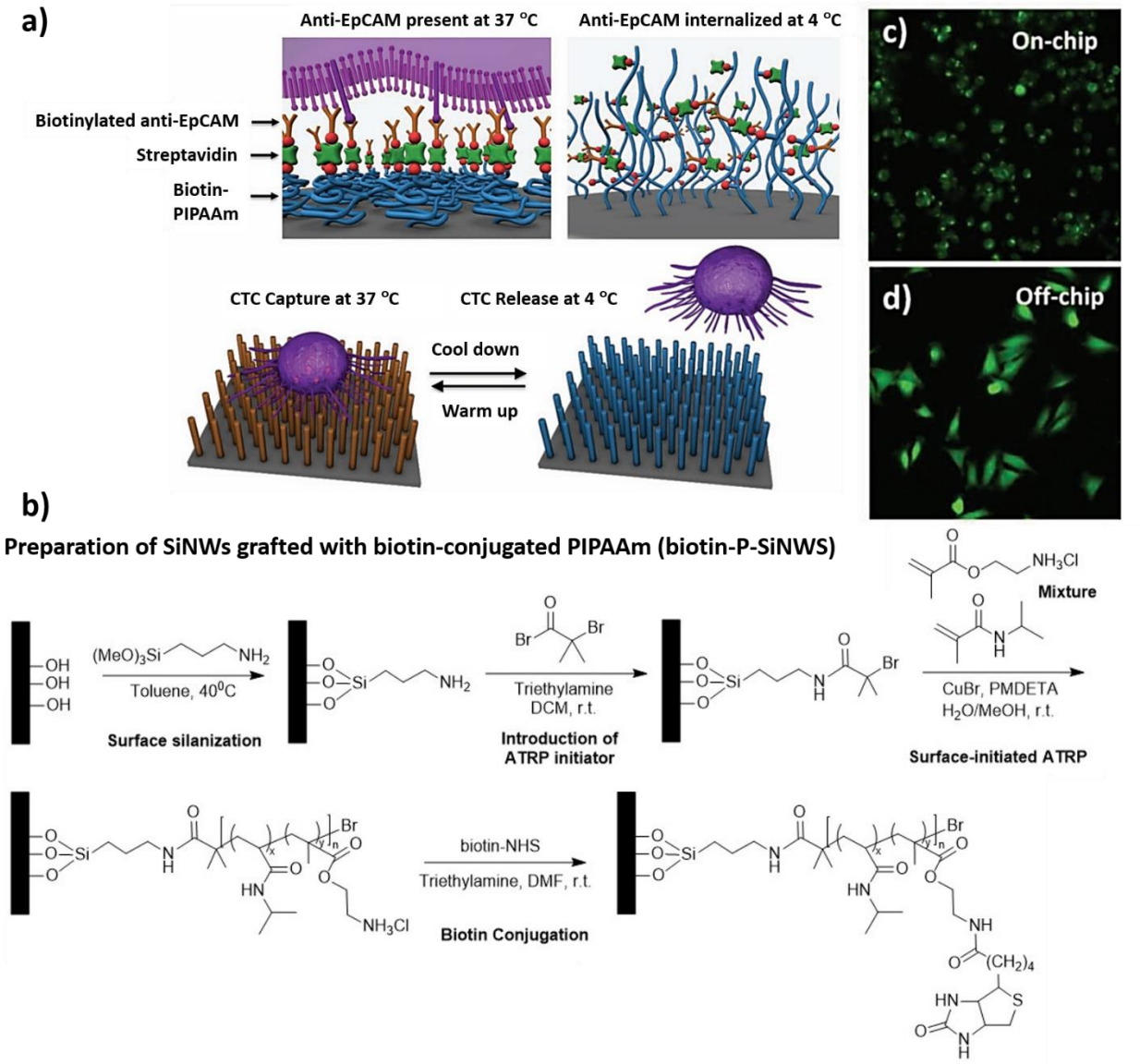

Figure 23: **a)** Conceptual illustration of capturing CTCs followed by their release upon stimulation at a reduced temperature. Thermal responsiveness was conferred onto silicon nanowire substrate (SiNWS) by covalently grafting with biotin-functionalized polymer brushes (i.e., PNIPAM); **b)** Conjugations reactions involved in the preparation of SiNWs grafted with biotin-conjugated PNIPAM; **c)** MCF7 cells cultured after cell capture and **d)** successful release from anti-EpCAM coated biotin-P-SiNWS at 4°C with retained functionality. Adapted from ref.[169]

A similar report where silicon nanostructured platform (Click Chip) was developed by integrating biorthogonal ligation mediated CTC capture with disulfide cleavage-driven CTC release.[170] Dong et al. demonstrated that instead of the commonly used anti-EpCAM enriched CTC immobilization methods, click chemistry components, i.e., tetrazine (Tz) and *trans*-cyclooctene (TCO), could be grafted on cell capturing device and on CTCs, respectively. The interactions of Tz-grafted SiNWS with TCO-grafted CTCs were higher, irreversible, and insensitive to biomolecules, water, and oxygen.[171] This chemo-specific reaction improved the CTC capture efficiency with well-preserved

mRNA while reducing nonspecific immobilization of WBCs. Next to CTC capture, exposure to a disulfide cleavage agent (DTT) resulted in the rapid CTC release from the SiNWS by cleavage of the disulfide bond enriched between the Tz to the SiNWS. In comparison, the Click Chips proved to be highly efficient with an overall capture efficiency of 94 ± 3% in spite of using a lower quantity of TCO-anti-EpCAM (as low as 0.1 ng) per capture study compared to with previous NanoVelcro Chips, which used 200 ng anti-EpCAM.

Intravascular CTC capture (in vivo/ ex vivo flow-through system)

Almost all the CTC capture methodologies described above are limited to lesser blood volumes (1-100 mL); therefore, the number of captured CTCs is lower. The ability to examine larger blood volumes might enhance the number of CTCs available for enumeration, which would ultimately increase the statistical confidence of sampling for comparison and further biological characterization.[172] On the other hand, several *in vivo* technologies have been described to overcome the limit in using small blood volume. For example, CellCollector involves a structured, functionalized stainless-steel medical-grade wire that offers the opportunity of isolating CTCs from the circulating blood of a patient in a significantly high number, under the largest blood flow volume. The medical wire preparation involved plating with a 2 µm thick gold layer deposited by galvanization, followed by a hydrogel layer of synthetic polycarboxylate grafted to the gold layer. Finally, the carboxyl group functionalities present in the hydrogel were used for conjugation with the anti-EpCAM antibody (CD326) via carbodiimide crosslinking chemistry. The wire coated with EpCAM antibodies was introduced in the arm vein of cancer patients and was subjected for 30 minutes, where EpCAM$^+$ cells can bind to the device (**Figure 24**). Captured CTCs were identified by staining for EpCAM, keratins, and nuclear counterstain was done using Hoechst33342 with CD45 staining necessary to eliminate false-positive events (i.e., leukocytes). This technique has shown a high detection rate in several cancers, including lung, prostate, breast, and neuroendocrine.[121, 173-177] In fifty lung cancer patients, 185 in vivo applications were performed, out of which 108 wires were positive of >1 CTCs, with 20 wires showing the presence of CTC clusters.[173]

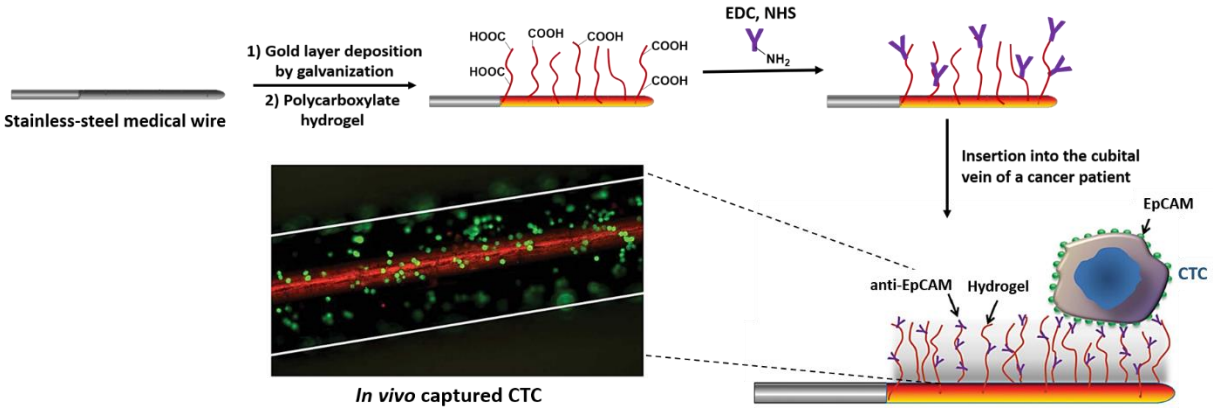

Figure 24: a) Schematic drawing of the functionalized tip of medical wire. Anti-EpCAM molecules conjugated to polycarboxylate hydrogel (1–5 µm thickness), which is coated onto gold-plated (200 nm) Seldinger guidewire. This medical wire interacts with CTCs expressing EpCAM antigen, e.g., CTC of breast and lung cancer patients; **b)** SK-BR-3 breast cancer cells captured on the wire

stained with FITC-labeled antibodies (green). The white lines denote the borders of the wire. Adapted from ref.[121]

A different approach for *in vivo* capture of NSCLC cells by MagWIRE (magnetic wire for intravascular retrieval and enrichment) was reported by Vermesh et al. .[178] Here, MagWIRE was inserted in Porcine auricular vein, and H1650 cells (1 mL) at concentrations ranging from 2,500 to 10,000 cells mL^{-1} and 1 mL of 2 mg mL^{-1} Dynabeads were manually injected through 22-gauge catheters over the course for 1 min in Porcine models. The MagWIRE was removed from the auricular vein, and the MagWIRE was visibly coated with MPs. MagWIRE captured the H1650 cells with 1 to 8% efficiency for 2,500-10,000 cells related to a 10-80 fold upgrading compared with a 5 mL blood draw.
However, this approach requires pre-injection of EpCAM coated magnetic particles of alternating polarity to label CTCs, limiting its long-term usage due to possible systemic overexposure of magnetic iron nanoparticles.

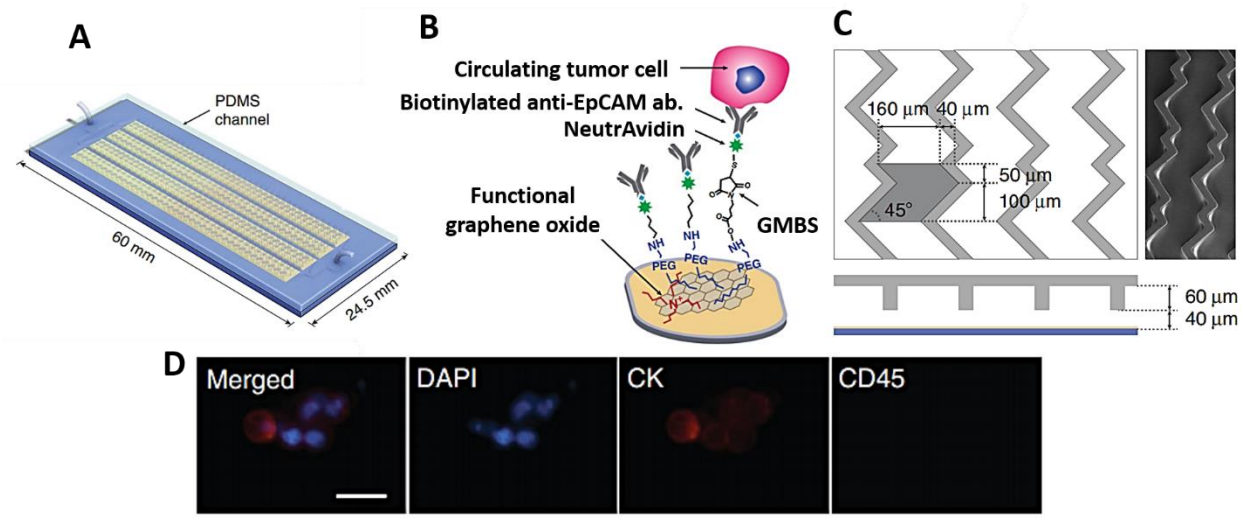

Figure 25: Ex vivo evaluation of HBGO chip for CTC capture. **A-B)** Schematic of the HBGO chip and the conjugation chemistry between functional GO and anti-EpCAM antibody**; C)** Schematic and micrograph of the herringbone grooved channel geometry; **D)** Fluorescent microscope image of MCF7 cells and clusters captured ex vivo, stained with DAPI (blue), Cytokeratin (red), and CD45 (green). The scale bars denote 25 µm. Adapted from ref.[178]

Kim et al. have designed an *ex vivo* portable indwelling intravascular aphaeretic CTC monitoring tool. It can be worn by a patient for several hours to interrogate a large volume of blood (**Figure 25**).[179] The microfluidic design consisted of silicon dioxide substrate patterned with a gold thin film layer bonded to PDMS structure containing microchannels with herringbone grooves to allow tumultuous mixing at low Reynold number. Functional GO sheets were assembled onto the gold layer expressing high-density EpCAM antibodies on the substrate surface through PEG crosslinkers. The system has been validated first on human breast cancer MCF7 cells followed by *in vivo* animal experiments on dogs injected with non-labeled MCF-7 cells. The maximal efficiency (> 90%) could be achieved at a flow rate of 1 mL/h (≈ 16.67 µL/min), which dropped on increasing

the flowrate. After CTC enrichment, the system returned the remaining blood to the body, and the system was capable of screening 1-2% of the whole blood over 2 h.

Xie et al. and co-workers published an *in vivo* methodology to capture and downregulate colorectal CTCs, which might lead to metastasis prevention in cancer survivors after surgery.[180, 181] The reported system consisted of surface-functionalized PAMAM dendrimers as a scaffold to accommodate a cocktail of antibodies (anti-EpCAM and antiSlex antibodies) to capture cancer cells in harmony (HT29 colorectal cell line used as CTC model). To evaluate the capturing effects of the conjugates using HT29 cells, anti-EpCAM and antiSlex were linked to phycoerythrin (PE, orange fluorescence) and Fluorescein isothiocyanate (FITC, green fluorescence), respectively. CTCs were captured from mice blood when cancer cells and PAMAM-dual antibody conjugates were injected into the nude mice. High capture efficiency and specificity were observed with dual antibody conjugates compared to its single antibody conjugate for HT29 cells.

There still exist some caveats of the *in vivo cell* enrichment approach that includes the requirement of a long time to ensure maximal blood flows over the vein indwelling needle for CTC capture. Also, the cost of the system is high, as CTC capture is dependent on antibodies.

4. Conclusions / future prospective

This review primarily focused on advanced materials and chemo-specific designs at the nano/micrometer scale in isolating circulating tumor cells (CTCs). The development of advanced materials for next-generation, clinically relevant technologies reshapes the medical landscape, both from the clinician's and patient's perspectives. Moreover, when confronted with the burden of diseases like cancer and concomitant mortality from metastatic progression, it is prudent to emphasize the urgent requirement for timely diagnosis that can directly impact crucial prognostic and treatment decisions. To that end, considerable basic and clinical research is focused on developing future, commercially viable, diagnostic, and theranostic tools to aid in cancer disease management.

A wide range of materials from the nano to micrometer scale has been designed and chemically tuned to offer exceptional sensitivity and selectivity for isolating rare tumorigenic cells, like CTCs, from cancer patient's peripheral blood using liquid biopsy methods, thereby providing a real-time snapshot of the disease status. This review primarily detailed the chemo-functionalities and structure-activity relationship of advanced material substrates involved in the generation of chemo-specific substrates conjugated to CTC surface tumor-specific targeting ligands. Currently, the method of choice of CTC isolation employs highly magnetic, low nonspecific binding, colloidal magnetic particles, which are easily manipulated using an external magnetic field. Furthermore, the utility of magnetic-assisted, multi-component chemo designs involving ligand-based nanogels, cellulose systems, and micro-rockets offer CTC capture with higher efficiencies from a mixed population of nucleated cells.

The multicomponent platforms provide synergistic augmented multivalences and a high density of targeting units per molecules for efficient ligand-receptor interactions. Lately, the amount of antibody conjugated to nanoparticles used per mL of blood is extremely high, making the process expensive. In contrast, fluidic systems can be directly functionalized with a very low amount of targeting ligand and integrated with nanomaterial. Such chemo-dynamic systems allow maximal receptor-target interaction by controlling the residence time of blood containing CTCs.

Since it is clinically relevant to study molecular and functional read-outs post CTC capture, the chemo design is equipped with linkers/targeting ligands to release CTCs without disrupting their viability and functions. Other targeting ligands that bind to the cell surface like antibodies, such as transferrin, aptamers, folic acid, etc. should be implemented since they offer low manufacturing costs and better thermal stabilities.

It is noteworthy that while the biological interaction between the cell surface-expressed tumor biomarker and the respective capturing moiety is not easily manipulated, the material chemistry governing the systematic synthesis of the capture substrate is subject to a high degree of control and fine-tuning. To that end, the choice of the chemo-specific substrates, reactive linkers, and the chemical methodologies used for synthesizing CTC capture materials are crucial in ascertaining that the endpoint capture-moiety conjugated substrates are highly efficient and specific in their targeting. Furthermore, the review highlights the necessity for efficient and specific capture of CTCs and the downstream genomic advances utilized to identify, characterize, and classify the heterogenic nature of these metastatic seeds.

It is equally important to recognize that the breakthrough advances in material chemistry that make the abovementioned technologies possible, there is no 'one-solution-fits-all' method that offers comprehensive profiling of CTCs, due to their heterogenic nature. Thus, combinatorial and multicomponent strategies must be attempted to isolate CTCs with a greater limit of detection and high recovery rate, with the possibility of extracting genomic, proteomic, and artificial intelligence-based predictive analysis to reflect the accurate characteristics of the CTCs at a precise disease stage.

The advent of such technologies will mark a turning point in cancer disease management. More importantly, it must be maintained that while it is challenging to develop, both from the scientific as well as economic aspects, these game-changing technologies must be both accessible and affordable, particularly in developing countries, given that the burden of cancer affects individuals of all socio-economic strata globally.

5. Acknowledgments

The authors acknowledge the support from the Biotechnology Industry Research Assistance Council (BIRAC) Department of Biotechnology (DBT), GOI, Nanobiotechnology Research Grant from DBT, and Technology Infrastructure-Department of Science and Technology (FIST-DST) and IKERBASQUE-Basque Foundation for Science. The authors thank Aravindan Vasudevan for proofreading the manuscript.

6. Conflicts of interest

No conflict of interest was declared.

7. References

1. L. Fusco, A. Gazzi, G. Peng, Y. Shin, S. Vranic, D. Bedognetti, F. Vitale, A. Yilmazer, X. Feng, B. Fadeel, C. Casiraghi and L. G. Delogu, *Theranostics*, 2020, **10**, 5435-5488.
2. L. Cheng, X. Wang, F. Gong, T. Liu, and Z. Liu, *Advanced Materials*, 2020, **32**, 1902333.
3. G. Nagel, A. Sousa-Herves, S. Wedepohl and M. Calderón, *Theranostics*, 2020, **10**, 91-108.
4. P. Ray, M. Ferraro, R. Haag and M. Quadir, *Macromolecular Bioscience*, 2019, **19**, 1900073.
5. J. Shi, A. R. Votruba, O. C. Farokhzad and R. Langer, *Nano Letters*, 2010, **10**, 3223-3230.

6. S. Correa, K. Y. Choi, E. C. Dreaden, K. Renggli, A. Shi, L. Gu, K. E. Shopsowitz, M. A. Quadir, E. Ben-Akiva and P. T. Hammond, *Advanced Functional Materials*, 2016, **26**, 991-1003.
7. D. Gao, X. Guo, X. Zhang, S. Chen, Y. Wang, T. Chen, G. Huang, Y. Gao, Z. Tian and Z. Yang, *Materials Today Bio*, 2020, **5**, 100035.
8. M. Molina, M. Asadian-Birjand, J. Balach, J. Bergueiro, E. Miceli and M. Calderón, *Chemical Society Reviews*, 2015, **44**, 6161-6186.
9. S. S. Banerjee, G. V. Khutale, V. Khobragade, N. R. Kale, M. Pore, G. P. Chate, A. Jalota-Badhwar, M. Dongare and J. J. Khandare, *Advanced Materials Interfaces*, 2017, **4**.
10. J. T. Connelly, J. P. Rolland and G. M. Whitesides, *Analytical Chemistry*, 2015, **87**, 7595-7601.
11. J. J. Khandare, S. Jayant, A. Singh, P. Chandna, Y. Wang, N. Vorsa and T. Minko, *Bioconjugate Chemistry*, 2006, **17**, 1464-1472.
12. M. Calderón, M. A. Quadir, S. K. Sharma and R. Haag, *Advanced Materials*, 2010, **22**, 190-218.
13. M. W. Kulka, I. S. Donskyi, N. Wurzler, D. Salz, Ö. Özcan, W. E. S. Unger and R. Haag, *ACS Applied Bio Materials*, 2019, **2**, 5749-5759.
14. J. J. Khandare, P. Chandna, Y. Wang, V. P. Pozharov and T. Minko, *Journal of Pharmacology and Experimental Therapeutics*, 2006, **317**, 929.
15. R. Raman and R. Langer, *Advanced Materials*, 2020, **32**, 1901969.
16. G. M. Whitesides, *Nature Biotechnology*, 2003, **21**, 1161-1165.
17. R. Duncan and M. J. Vicent, *Advanced Drug Delivery Reviews*, 2013, **65**, 60-70.
18. N.-Y. Lee, W.-C. Ko and P.-R. Hsueh, *Front Pharmacol*, 2019, **10**, 1153-1153.
19. H. Khurshid, B. Friedman, B. Berwin, Y. Shi, D. B. Ness and J. B. Weaver, *AIP Adv*, 2017, **7**, 056723-056723.
20. Q. Liu, Y.-C. Yeh, S. Rana, Y. Jiang, L. Guo and V. M. Rotello, *Cancer Lett*, 2013, **334**, 196-201.
21. *Nature Cancer*, 2020, **1**, 1-2.
22. F. Bray, J. Ferlay, I. Soerjomataram, R. L. Siegel, L. A. Torre and A. Jemal, *CA: A Cancer Journal for Clinicians*, 2018, **68**, 394-424.
23. L. The, *The Lancet*, 2018, **392**, 985.
24. P. Chaturvedi, A. Singh, C.-Y. Chien and S. Warnakulasuriya, *BMJ*, 2019, **365**, l2142.
25. D. Hanahan and R. A. Weinberg, *Cell*, 2000, **100**, 57-70.
26. H. Dillekås, M. S. Rogers and O. Straume, *Cancer Med*, 2019, **8**, 5574-5576.
27. P. S. Steeg, *Nature Reviews Cancer*, 2016, **16**, 201-218.
28. D. Yao, C. Dai and S. Peng, *Molecular Cancer Research*, 2011, **9**, 1608.
29. F. Nurwidya, J. Zaini, A. C. Putra, S. Andarini, A. Hudoyo, E. Syahruddin and F. Yunus, *Chonnam Med J*, 2016, **52**, 151-158.
30. T. P. Butler and P. M. Gullino, *Cancer Research*, 1975, **35**, 512.
31. Y. S. Chang, E. di Tomaso, D. M. McDonald, R. Jones, R. K. Jain and L. L. Munn, *Proc Natl Acad Sci U S A*, 2000, **97**, 14608-14613.
32. T. Lozar, K. Gersak, M. Cemazar, C. G. Kuhar and T. Jesenko, *Radiol Oncol*, 2019, **53**, 131-147.
33. J. Khandare, B. N. Qayyumi, A. Bharde, G. Aland, A. Sagare, S. Tripathi, N. Singh, S. Jayant, A. Muglikar, R. Badave, A. Vasudevan, K. Prabhash and P. Chaturvedi, *Clinical Cancer Research*, 2020, **26**, B30.
34. J. Khandare, B. Qayyumi, A. Bharde, G. Aland, S. Jayant, S. Tripathi, N. Singh, R. Badave, A. D'Souza, B. Singh, S. Arora, N. Kale, A. Vasudevan, A. Ashturkar, K. Prabhash and P. Chaturvedi, *Journal of Clinical Oncology*, 2020, **38**, e15541-e15541.
35. M. G. Krebs, R. L. Metcalf, L. Carter, G. Brady, F. H. Blackhall and C. Dive, *Nature Reviews Clinical Oncology*, 2014, **11**, 129-144.
36. https://www.roche.com/media/releases/med-cor-2020-08-28.htm).
37. J. Khandare, B. N. Qayyumi, A. Bharde, G. Aland, S. Jayant, S. Tripathi, N. Singh, R. Badwe, A. Souza, B. Singh, S. Arora, N. Kale, A. Vasudevan, K. Prabhash and P. Chaturvedi, *Cancer Research*, 2020, **80**, LB-148.
38. J. P. Thiery, *Nature Reviews Cancer*, 2002, **2**, 442-454.
39. N. Aceto, A. Bardia, D. T. Miyamoto, M. C. Donaldson, B. S. Wittner, J. A. Spencer, M. Yu, A. Pely, A. Engstrom, H. Zhu, B. W. Brannigan, R. Kapur, S. L. Stott, T. Shioda, S. Ramaswamy, D. T. Ting, C. P. Lin, M. Toner, D. A. Haber and S. Maheswaran, *Cell*, 2014, **158**, 1110-1122.
40. I. J. Fidler, *JNCI: Journal of the National Cancer Institute*, 1970, **45**, 773-782.
41. T. R. Ashworth, *Aust Med J.*, 1869, **14**, 146.

42. K. Andree, G. Dalum and L. Terstappen, *Mol Oncol*, 2015, **10**.
43. H. K. Brown, M. Tellez-Gabriel, P.-F. Cartron, F. M. Vallette, M.-F. Heymann and D. Heymann, *Drug Discovery Today*, 2019, **24**, 763-772.
44. M. M. Ferreira, V. C. Ramani and S. S. Jeffrey, *Mol Oncol*, 2016, **10**, 374-394.
45. E. Rossi and R. Zamarchi, *Frontiers in genetics*, 2019, **10**, 958-958.
46. I. S. Batth, A. Mitra, S. Manier, I. M. Ghobrial, D. Menter, S. Kopetz and S. Li, *Ann Oncol*, 2017, **28**, 468-477.
47. S.-m. Park, D. J. Wong, C. C. Ooi, D. M. Kurtz, O. Vermesh, A. Aalipour, S. Suh, K. L. Pian, J. J. Chabon, S. H. Lee, M. Jamali, C. Say, J. N. Carter, L. P. Lee, W. G. Kuschner, E. J. Schwartz, J. B. Shrager, J. W. Neal, H. A. Wakelee, M. Diehn, V. S. Nair, S. X. Wang and S. S. Gambhir, *Proceedings of the National Academy of Sciences*, 2016, **113**, E8379.
48. Q. Wang, L. Zhao, L. Han, X. Tuo, S. Ma, Y. Wang, X. Feng, D. Liang, C. Sun, Q. Wang, Q. Song and Q. Li, *Journal*, 2019, **15**, 21-29.
49. M. J. M. Magbanua, H. S. Rugo, D. M. Wolf, L. Hauranieh, R. Roy, P. Pendyala, E. V. Sosa, J. H. Scott, J. S. Lee, B. Pitcher, T. Hyslop, W. T. Barry, S. J. Isakoff, M. Dickler, van, L. t Veer and J. W. Park, *Clinical Cancer Research*, 2018, **24**, 1486.
50. H. Tada, H. Takahashi, Y. Kuwabara-Yokobori, M. Shino and K. Chikamatsu, *Oral Oncol*, 2020, **102**, 104558.
51. S. Y. Lin, S.-C. Chang, S. Lam, R. Irene Ramos, K. Tran, S. Ohe, M. P. Salomon, A. A. S. Bhagat, C. Teck Lim, T. D. Fischer, L. J. Foshag, C. L. Boley, S. J. O'Day and D. S. B. Hoon, *Clin Chem*, 2020, **66**, 169-177.
52. C. Koch, A. Kuske, S. A. Joosse, G. Yigit, G. Sflomos, S. Thaler, D. J. Smit, S. Werner, K. Borgmann, S. Gärtner, P. Mossahebi Mohammadi, L. Battista, L. Cayrefourcq, J. Altmüller, G. Salinas-Riester, K. Raithatha, A. Zibat, Y. Goy, L. Ott, K. Bartkowiak, T. Z. Tan, Q. Zhou, M. R. Speicher, V. Müller, T. M. Gorges, M. Jücker, J.-P. Thiery, C. Brisken, S. Riethdorf, C. Alix-Panabières and K. Pantel, *EMBO Mol Med*, 2020, **12**, e11908-e11908.
53. S. L. Stott, R. J. Lee, S. Nagrath, M. Yu, D. T. Miyamoto, L. Ulkus, E. J. Inserra, M. Ulman, S. Springer, Z. Nakamura, A. L. Moore, D. I. Tsukrov, M. E. Kempner, D. M. Dahl, C.-L. Wu, A. J. Iafrate, M. R. Smith, R. G. Tompkins, L. V. Sequist, M. Toner, D. A. Haber and S. Maheswaran, *Sci Transl Med*, 2010, **2**, 25ra23-25ra23.
54. D. T. Miyamoto, R. J. Lee, S. L. Stott, D. T. Ting, B. S. Wittner, M. Ulman, M. E. Smas, J. B. Lord, B. W. Brannigan, J. Trautwein, N. H. Bander, C.-L. Wu, L. V. Sequist, M. R. Smith, S. Ramaswamy, M. Toner, S. Maheswaran and D. A. Haber, *Cancer Discovery*, 2012, **2**, 995.
55. K. Onidani, H. Shoji, T. Kakizaki, S. Yoshimoto, S. Okaya, N. Miura, S. Sekikawa, K. Furuta, C. T. Lim, T. Shibahara, N. Boku, K. Kato and K. Honda, *Cancer Sci*, 2019, **110**, 2590-2599.
56. FDA Approves New FoundationOne®Liquid CDx Companion Diagnostic Indications for Three Targeted Therapies That Treat Advanced Ovarian, Breast and Non-Small Cell Lung Cancer [news release]. , https://www.foundationmedicine.com/press-releases/d7f17f4f-ab71-4c2b-9b98-bb12df081de1).
57. D. A. Haber and V. E. Velculescu, *Cancer discovery*, 2014, **4**, 650-661.
58. J. Tie, Y. Wang, C. Tomasetti, L. Li, S. Springer, I. Kinde, N. Silliman, M. Tacey, H.-L. Wong, M. Christie, S. Kosmider, I. Skinner, R. Wong, M. Steel, B. Tran, J. Desai, I. Jones, A. Haydon, T. Hayes, T. J. Price, R. L. Strausberg, L. A. Diaz, Jr., N. Papadopoulos, K. W. Kinzler, B. Vogelstein and P. Gibbs, *Sci Transl Med*, 2016, **8**, 346ra392-346ra392.
59. K. Pantel and C. Alix-Panabières, *Nature Reviews Clinical Oncology*, 2019, **16**, 409-424.
60. A. A. Chaudhuri, J. J. Chabon, A. F. Lovejoy, A. M. Newman, H. Stehr, T. D. Azad, M. S. Khodadoust, M. S. Esfahani, C. L. Liu, L. Zhou, F. Scherer, D. M. Kurtz, C. Say, J. N. Carter, D. J. Merriott, J. C. Dudley, M. S. Binkley, L. Modlin, S. K. Padda, M. F. Gensheimer, R. B. West, J. B. Shrager, J. W. Neal, H. A. Wakelee, B. W. Loo, Jr., A. A. Alizadeh and M. Diehn, *Cancer discovery*, 2017, **7**, 1394-1403.
61. Y.-Q. Li, B. K. Chandran, C. T. Lim and X. Chen, *Advanced Science*, 2015, **2**, 1500118.
62. Y. Ming, Y. Li, H. Xing, M. Luo, Z. Li, J. Chen, J. Mo and S. Shi, *Front Pharmacol*, 2017, **8**, 35.
63. S. Bhana, Y. Wang and X. Huang, *Nanomedicine (Lond)*, 2015, **10**, 1973-1990.
64. D. Nordmeyer, P. Stumpf, D. Gröger, A. Hofmann, S. Enders, S. B. Riese, J. Dernedde, M. Taupitz, U. Rauch, R. Haag, E. Rühl and C. Graf, *Nanoscale*, 2014, **6**, 9646-9654.
65. S. Kumar and S. H. Parekh, *Communications Chemistry*, 2020, **3**, 8.
66. C. Ge, J. Du, L. Zhao, L. Wang, Y. Liu, D. Li, Y. Yang, R. Zhou, Y. Zhao, Z. Chai and C. Chen, *Proc Natl Acad Sci U S A*, 2011, **108**, 16968-16973.
67. E. Fleige, M. A. Quadir and R. Haag, *Advanced Drug Delivery Reviews*, 2012, **64**, 866-884.
68. D. Sun, Z. Chen, M. Wu and Y. Zhang, *Nanotheranostics*, 2017, **1**, 389-402.

69. J. Cheng, Y. Liu, Y. Zhao, L. Zhang, L. Zhang, H. Mao and C. Huang, *Micromachines (Basel)*, 2020, **11**, 774.
70. Z. Li and G.-Y. Chen, *Nanomaterials (Basel)*, 2018, **8**, 278.
71. G. Pereira, C. A. P. Monteiro, G. M. Albuquerque, M. I. A. Pereira, M. P. Cabrera, P. E. Cabral Filho, G. A. L. Pereira, A. Fontesa and B. S. Santos, *Journal of the Brazilian Chemical Society*, 2019, **30**, 2536-2561.
72. Y. Wan, Y. Liu, P. B. Allen, W. Asghar, M. A. I. Mahmood, J. Tan, H. Duhon, Y.-t. Kim, A. D. Ellington and S. M. Iqbal, *Lab Chip*, 2012, **12**, 4693-4701.
73. J. Wang, M. Muto, R. Yatabe, T. Onodera, M. Tanaka, M. Okochi and K. Toko, *Sensors (Basel)*, 2017, **17**, 2249.
74. M. Abdolahi, D. Shahbazi-Gahrouei, S. Laurent, C. Sermeus, F. Firozian, B. J. Allen, S. Boutry and R. N. Muller, *Contrast Media & Molecular Imaging*, 2013, **8**, 175-184.
75. K. E. Fischer, B. J. Alemán, S. L. Tao, R. H. Daniels, E. M. Li, M. D. Bünger, G. Nagaraj, P. Singh, A. Zettl and T. A. Desai, *Nano Letters*, 2009, **9**, 716-720.
76. A. S. G. Curtis and M. Varde, *JNCI: Journal of the National Cancer Institute*, 1964, **33**, 15-26.
77. W. F. Liu and C. S. Chen, *Advanced drug delivery reviews*, 2007, **59**, 1319-1328.
78. P.-Y. Yeh, Y.-R. Chen, C.-F. Wang and Y.-C. Chang, *Biomacromolecules*, 2018, **19**, 426-437.
79. J. H. Myung, K. A. Gajjar, J. Saric, D. T. Eddington and S. Hong, *Angew Chem Int Ed Engl*, 2011, **50**, 11769-11772.
80. Q. Shen, L. Xu, L. Zhao, D. Wu, Y. Fan, Y. Zhou, W.-H. OuYang, X. Xu, Z. Zhang, M. Song, T. Lee, M. A. Garcia, B. Xiong, S. Hou, H.-R. Tseng and X. Fang, *Advanced Materials*, 2013, **25**, 2368-2373.
81. N.-N. Lu, M. Xie, J. Wang, S.-W. Lv, J.-S. Yi, W.-G. Dong and W.-H. Huang, *ACS Applied Materials & Interfaces*, 2015, **7**, 8817-8826.
82. N. Sun, M. Liu, W. Jine, W. Zhili, X. Li, B. Jiang and R. Pei, *Small*, 2016, **12**.
83. A. Zamay, G. Zamay, O. Kolovskaya, T. Zamay and M. Berezovski, 2017, vol. 994, pp. 67-81.
84. P. Ding, Z. Wang, Z. Wu, W. Zhu, L. Liu, N. Sun and R. Pei, *Journal of Materials Chemistry B*, 2020, **8**, 3408-3422.
85. L. Wu, L. Zhu, M. Huang, J. Song, H. Zhang, Y. Song, W. Wang and C. Yang, *TrAC Trends in Analytical Chemistry*, 2019, **117**, 69-77.
86. Y. Song, Z. Zhu, Y. An, W. Zhang, H. Zhang, D. Liu, C. Yu, W. Duan and C. J. Yang, *Analytical Chemistry*, 2013, **85**, 4141-4149.
87. D.-L. Wang, Y.-L. Song, Z. Zhu, X.-L. Li, Y. Zou, H.-T. Yang, J.-J. Wang, R.-J. Pan, C. Yang and D.-Z. Kang, *Biochemical and Biophysical Research Communications*, 2014, **453**.
88. D. Shangguan, Y. Li, Z. Tang, Z. C. Cao, H. W. Chen, P. Mallikaratchy, K. Sefah, C. J. Yang and W. Tan, *Proc Natl Acad Sci U S A*, 2006, **103**, 11838-11843.
89. C. S. M. Ferreira, C. S. Matthews and S. Missailidis, *Tumor Biology*, 2006, **27**, 289-301.
90. C. Raimondi, C. Nicolazzo and A. Gradilone, *Chin J Cancer Res*, 2015, **27**, 461-470.
91. U. Schnell, V. Cirulli and B. N. G. Giepmans, *Biochimica et Biophysica Acta (BBA) - Biomembranes*, 2013, **1828**, 1989-2001.
92. Z. Eslami-S, L. E. Cortés-Hernández and C. Alix-Panabières, *Cells*, 2020, **9**, 1836.
93. G. Spizzo, P. Obrist, C. Ensinger, I. Theurl, M. Dünser, A. Ramoni, E. Gunsilius, G. Eibl, G. Mikuz and G. Gastl, *International Journal of Cancer*, 2002, **98**, 883-888.
94. M. Varga, P. Obrist, S. Schneeberger, G. Mühlmann, C. Felgel-Farnholz, D. Fong, M. Zitt, T. Brunhuber, G. Schäfer, G. Gastl and G. Spizzo, *Clinical Cancer Research*, 2004, **10**, 3131.
95. P. Scheunemann, N. H. Stoecklein, A. Rehders, M. Bidde, S. Metz, M. Peiper, C. F. Eisenberger, J. Schulte Am Esch, W. T. Knoefel and S. B. Hosch, *Langenbecks Arch Surg*, 2008, **393**, 359-365.
96. *United States Pat.,* US6365362B1, 1999.
97. *United States Pat.,* US6623982B1, 1999.
98. D. L. Adams, S. Stefansson, C. Haudenschild, S. S. Martin, M. Charpentier, S. Chumsri, M. Cristofanilli, C.-M. Tang and R. K. Alpaugh, *Cytometry Part A*, 2015, **87**, 137-144.
99. H. Wang, N. H. Stoecklein, P. P. Lin and O. Gires, *Oncotarget*, 2017, **8**, 1884-1912.
100. M. Zeisberg and E. G. Neilson, *J Clin Invest*, 2009, **119**, 1429-1437.
101. S. Ménard, S. M. Pupa, M. Campiglio and E. Tagliabue, *Oncogene*, 2003, **22**, 6570-6578.
102. J. Peng, Q. Zhao, W. Zheng, W. Li, P. Li, L. Zhu, X. Liu, B. Shao, H. Li, C. Wang and Y. Yang, *ACS Applied Materials & Interfaces*, 2017, **9**, 18423-18428.

103. M. M. Moasser, *Oncogene*, 2007, **26**, 6469-6487.
104. L. Nie, F. Li, X. Huang, Z. P. Aguilar, Y. A. Wang, Y. Xiong, F. Fu and H. Xu, *ACS Applied Materials & Interfaces*, 2018, **10**, 14055-14062.
105. L. E. Kelemen, *International Journal of Cancer*, 2006, **119**, 243-250.
106. T. R. Daniels, T. Delgado, J. A. Rodriguez, G. Helguera and M. L. Penichet, *Clinical Immunology*, 2006, **121**, 144-158.
107. C. Biglione, J. Bergueiro, M. Asadian-Birjand, C. Weise, V. Khobragade, G. Chate, M. Dongare, J. Khandare, M. C. Strumia and M. Calderón, *Polymers (Basel)*, 2018, **10**, 174.
108. S. S. Banerjee, A. Jalota-Badhwar, S. D. Satavalekar, S. G. Bhansali, N. D. Aher, R. R. Mascarenhas, D. Paul, S. Sharma and J. J. Khandare, *Advanced Healthcare Materials*, 2013, **2**, 800-805.
109. S. S. Banerjee, A. Jalota-Badhwar, K. R. Zope, K. J. Todkar, R. R. Mascarenhas, G. P. Chate, G. V. Khutale, A. Bharde, M. Calderon and J. J. Khandare, *Nanoscale*, 2015, **7**, 8684-8688.
110. R. S. Hazra, N. Kale, G. Aland, B. Qayyumi, D. Mitra, L. Jiang, D. Bajwa, J. Khandare, P. Chaturvedi and M. Quadir, *Scientific Reports*, 2020, **10**, 10010.
111. S. S. Banerjee, G. V. Khutale, V. Khobragade, N. R. Kale, M. Pore, G. P. Chate, A. Jalota-Badhwar, M. Dongare and J. J. Khandare, *Advanced Materials Interfaces*, 2017, **4**, 1600934.
112. C. Ding, C. Zhang, X. Yin, X. Cao, M. Cai and Y. Xian, *Analytical Chemistry*, 2018, **90**, 6702-6709.
113. L. Bai, Y. Du, J. Peng, Y. Liu, Y. Wang, Y. Yang and C. Wang, *J. Mater. Chem. B*, 2014, **2**.
114. X. Zhou, B. Luo, K. Kang, S. Ma, X. Sun, F. Lan, Q. Yi and Y. Wu, *Journal of Materials Chemistry B*, 2019, **7**, 393-400.
115. Y. Xiao, L. Lin, M. Shen and X. Shi, *Bioconjugate Chemistry*, 2020, **31**, 130-138.
116. J. H. Myung, K. A. Gajjar, J. Saric, D. T. Eddington and S. Hong, *Angewandte Chemie International Edition*, 2011, **50**, 11769-11772.
117. J. B. Haun, N. K. Devaraj, S. A. Hilderbrand, H. Lee and R. Weissleder, *Nature Nanotechnology*, 2010, **5**, 660-665.
118. X. Li, J. Chen, H. Liu, Z. Deng, J. Li, T. Ren, L. Huang, W. Chen, Y. Yang and S. Zhong, *Colloids and Surfaces B: Biointerfaces*, 2019, **181**, 379-388.
119. J. Chen, L. Yu, Y. Li, J. L. Cuellar-Camacho, Y. Chai, D. Li, Y. Li, H. Liu, L. Ou, W. Li and R. Haag, *Advanced Functional Materials*, 2019, **29**, 1808961.
120. K. C. Andree, A. M. C. Barradas, A. T. Nguyen, A. Mentink, I. Stojanovic, J. Baggerman, J. van Dalum, C. J. M. van Rijn and L. W. M. M. Terstappen, *ACS Applied Materials & Interfaces*, 2016, **8**, 14349-14356.
121. N. Saucedo-Zeni, S. Mewes, R. Niestroj, L. Gasiorowski, D. Murawa, P. Nowaczyk, T. Tomasi, E. Weber, G. Dworacki, N. G. Morgenthaler, H. Jansen, C. Propping, K. Sterzynska, W. Dyszkiewicz, M. Zabel, M. Kiechle, U. Reuning, M. Schmitt and K. Lücke, *Int J Oncol*, 2012, **41**, 1241-1250.
122. S. Kim, K.-R. Shin and B.-T. Zhang, *Molecular immunocomputing with application to alphabetical pattern recognition mimics the characterization of ABO blood type*, 2004.
123. S. Riethdorf, L. O'Flaherty, C. Hille and K. Pantel, *Advanced Drug Delivery Reviews*, 2018, **125**, 102-121.
124. R. Massart, *IEEE Transactions on Magnetics*, 1981, **17**, 1247-1248.
125. J. Lee, T. Isobe and M. Senna, *Colloids and Surfaces A: Physicochemical and Engineering Aspects*, 1996, **109**, 121-127.
126. S.-J. Lee, J.-R. Jeong, S. Shin, J.-C. Kim and J.-D. Kim, *Journal of Magnetism and Magnetic Materials*, 2004, **2829050**.
127. S. Sun and H. Zeng, *Journal of the American Chemical Society*, 2002, **124**, 8204-8205.
128. Z. Li, H. Chen, H. Bao and M. Gao, *Chemistry of Materials*, 2004, **16**.
129. J. Rockenberger, E. C. Scher and A. P. Alivisatos, *Journal of the American Chemical Society*, 1999, **121**, 11595-11596.
130. K. S. Suslick, M. Fang and T. Hyeon, *Journal of the American Chemical Society*, 1996, **118**, 11960-11961.
131. S. Yu and G. M. Chow, *J Nanosci Nanotechnol*, 2006, **6**, 2135-2140.
132. Z. Dai, F. Meiser and H. Möhwald, *Journal of Colloid and Interface Science*, 2005, **288**, 298-300.
133. T. González-Carreño, M. P. Morales, M. Gracia and C. J. Serna, *Materials Letters*, 1993, **18**, 151-155.
134. S. Veintemillas-Verdaguer, M. P. Morales and C. J. Serna, *Materials Letters*, 1998, **35**, 227-231.
135. M. P. Morales, O. Bomati-Miguel, R. Pérez de Alejo, J. Ruiz-Cabello, S. Veintemillas-Verdaguer and K. O'Grady, *Journal of Magnetism and Magnetic Materials*, 2003, **266**, 102-109.

136. T. Hyeon, *Chemical Communications*, 2003, DOI: 10.1039/B207789B, 927-934.
137. J. Wang, J. Sun, Q. Sun and Q. Chen, *Materials Research Bulletin*, 2003, **38**, 1113-1118.
138. Y.-h. Zheng, Y. Cheng, F. Bao and Y.-s. Wang, *Materials Research Bulletin*, 2006, **41**, 525-529.
139. B. Mao, Z. Kang, E. Wang, S. Lian, L. Gao, C. Tian and C. Wang, *Materials Research Bulletin*, 2006, **41**, 2226-2231.
140. J. G. Parsons, C. Luna, C. E. Botez, J. Elizalde and J. L. Gardea-Torresdey, *Journal of Physics and Chemistry of Solids*, 2009, **70**, 555-560.
141. F. Jiang, C. Wang, Y. Fu and R.-C. Liu, *Journal of Alloys and Compounds - J ALLOYS COMPOUNDS*, 2010, **503**.
142. *United States Pat.,* US 6,365,362 B1, 1999.
143. E. Racila, D. Euhus, A. J. Weiss, C. Rao, J. McConnell, L. W. Terstappen and J. W. Uhr, *Proc Natl Acad Sci U S A*, 1998, **95**, 4589-4594.
144. F. Herranz, B. Salinas, H. Groult, J. Pellico, A. V. Lechuga-Vieco, R. Bhavesh and J. Ruiz-Cabello, *Nanomaterials (Basel)*, 2014, **4**, 408-438.
145. *Europe Pat.,* 3259598, 2017.
146. L. M. Millner, M. W. Linder and R. Valdes, Jr., *Ann Clin Lab Sci*, 2013, **43**, 295-304.
147. Z. Shen, A. Wu and X. Chen, *Chemical Society reviews*, 2017, **46**, 2038-2056.
148. L. Muinelo-Romay, M. Vieito, A. Abalo, M. A. Nocelo, F. Barón, U. Anido, E. Brozos, F. Vázquez, S. Aguín, M. Abal and R. L. López, *Cancers (Basel)*, 2014, **6**, 153-165.
149. X.-X. Jie, X.-Y. Zhang and C.-J. Xu, *Oncotarget*, 2017, **8**, 81558-81571.
150. M. Asadian-Birjand, C. Biglione, J. Bergueiro, A. Cappelletti, C. Rahane, G. Chate, J. Khandare, B. Klemke, M. Strumia and M. Calderon, *Macromolecular rapid communications*, 2015, **37**.
151. M. Giulbudagian, M. Asadian-Birjand, D. Steinhilber, K. Achazi, M. Molina and M. Calderón, *Polymer Chemistry*, 2014, **5**, 6909-6913.
152. C. E. Chivers, A. L. Koner, E. D. Lowe and M. Howarth, *Biochem J*, 2011, **435**, 55-63.
153. N. Sun, M. Liu, J. Wang, Z. Wang, X. Li, B. Jiang and R. Pei, *Small*, 2016, **12**, 5090-5097.
154. Y. Zhang, B. S. Lai and M. Juhas, *Molecules*, 2019, **24**, 941.
155. V. Incani, C. Danumah and Y. Boluk, *Cellulose*, 2013, **20**, 191-200.
156. Y. Shi, A. Pramanik, C. Tchounwou, F. Pedraza, R. A. Crouch, S. R. Chavva, A. Vangara, S. S. Sinha, S. Jones, D. Sardar, C. Hawker and P. C. Ray, *ACS Applied Materials & Interfaces*, 2015, **7**, 10935-10943.
157. C. Garlisi and G. Palmisano, *Applied Surface Science*, 2017, **420**, 83-93.
158. R. Gertler, R. Rosenberg, K. Fuehrer, M. Dahm, H. Nekarda and J. R. Siewert, *Recent Results Cancer Res*, 2003, **162**, 149-155.
159. S. Ribeiro-Samy, M. I. Oliveira, T. Pereira-Veiga, L. Muinelo-Romay, S. Carvalho, J. Gaspar, P. P. Freitas, R. López-López, C. Costa and L. Diéguez, *Scientific Reports*, 2019, **9**, 8032.
160. E. Park, C. Jin, Q. Guo, R. Ang, S. Duffy, K. Matthews, A. Azad, H. Abdi, T. Todenhöfer, J. Bazov, K. Chi, P. Black and H. Ma, *Small (Weinheim an der Bergstrasse, Germany)*, 2016, **12**.
161. S. Riethdorf, H. Fritsche, V. Müller, T. Rau, C. Schindlbeck, B. Rack, W. Janni, C. Coith, K. Beck, F. Jänicke, S. Jackson, T. Gornet, M. Cristofanilli and K. Pantel, *Clinical Cancer Research*, 2007, **13**, 920.
162. H. J. Yoon, T. H. Kim, Z. Zhang, E. Azizi, T. M. Pham, C. Paoletti, J. Lin, N. Ramnath, M. S. Wicha, D. F. Hayes, D. M. Simeone and S. Nagrath, *Nature Nanotechnology*, 2013, **8**, 735-741.
163. T. H. Kim, H. J. Yoon, S. Fouladdel, Y. Wang, M. Kozminsky, M. L. Burness, C. Paoletti, L. Zhao, E. Azizi, M. S. Wicha and S. Nagrath, *Advanced Biosystems*, 2019, **3**, 1800278.
164. H. Wang, X. Wang, X. Li and H. Dai, *Nano Research*, 2009, **2**, 336-342.
165. L. Zhao, C. Tang, L. Xu, Z. Zhang, X. Li, H. Hu, S. Cheng, W. Zhou, M. Huang, A. Fong, B. Liu, H.-R. Tseng, H. Gao, Y. Liu and X. Fang, *Small (Weinheim an der Bergstrasse, Germany)*, 2016, **12**, 1072-1081.
166. M. Yu, A. Bardia, B. S. Wittner, S. L. Stott, M. E. Smas, D. T. Ting, S. J. Isakoff, J. C. Ciciliano, M. N. Wells, A. M. Shah, K. F. Concannon, M. C. Donaldson, L. V. Sequist, E. Brachtel, D. Sgroi, J. Baselga, S. Ramaswamy, M. Toner, D. A. Haber and S. Maheswaran, *Science*, 2013, **339**, 580.
167. S. Wang, K. Liu, J. Liu, Z. T. F. Yu, X. Xu, L. Zhao, T. Lee, E. K. Lee, J. Reiss, Y.-K. Lee, L. W. K. Chung, J. Huang, M. Rettig, D. Seligson, K. N. Duraiswamy, C. K. F. Shen and H.-R. Tseng, *Angewandte Chemie International Edition*, 2011, **50**, 3084-3088.

168. S. Nagrath, L. V. Sequist, S. Maheswaran, D. W. Bell, D. Irimia, L. Ulkus, M. R. Smith, E. L. Kwak, S. Digumarthy, A. Muzikansky, P. Ryan, U. J. Balis, R. G. Tompkins, D. A. Haber and M. Toner, *Nature*, 2007, **450**, 1235-1239.
169. S. Hou, H. Zhao, L. Zhao, Q. Shen, K. S. Wei, D. Y. Suh, A. Nakao, M. A. Garcia, M. Song, T. Lee, B. Xiong, S.-C. Luo, H.-R. Tseng and H.-h. Yu, *Advanced Materials*, 2013, **25**, 1547-1551.
170. J. Dong, Y. J. Jan, J. Cheng, R. Y. Zhang, M. Meng, M. Smalley, P.-J. Chen, X. Tang, P. Tseng, L. Bao, T.-Y. Huang, D. Zhou, Y. Liu, X. Chai, H. Zhang, A. Zhou, V. G. Agopian, E. M. Posadas, J.-J. Shyue, S. J. Jonas, P. S. Weiss, M. Li, G. Zheng, H.-H. Yu, M. Zhao, H.-R. Tseng and Y. Zhu, *Sci Adv*, 2019, **5**, eaav9186-eaav9186.
171. M. L. Blackman, M. Royzen and J. M. Fox, *Journal of the American Chemical Society*, 2008, **130**, 13518-13519.
172. A. L. Allan and M. Keeney, *Journal of Oncology*, 2010, **2010**, 426218.
173. T. M. Gorges, N. Penkalla, T. Schalk, S. A. Joosse, S. Riethdorf, J. Tucholski, K. Lücke, H. Wikman, S. Jackson, N. Brychta, O. von Ahsen, C. Schumann, T. Krahn and K. Pantel, *Clinical Cancer Research*, 2016, **22**, 2197.
174. C. Chudak, J. Herrmann and T. Lesser, *Journal of Thoracic Oncology*, 2016, **11**, S104-S105.
175. G. Theil, K. Fischer, E. Weber, R. Medek, R. Hoda, K. Lücke and P. Fornara, *PLoS One*, 2016, **11**, e0158354-e0158354.
176. Y. He, J. Shi, G. Shi, X. Xu, Q. Liu, C. Liu, Z. Gao, J. Bai and B. Shan, *Scientific Reports*, 2017, **7**, 9542.
177. D. Mandair, C. Vesely, L. Ensell, H. Lowe, V. Spanswick, J. A. Hartley, M. E. Caplin and T. Meyer, *Endocrine-Related Cancer*, 2016, **23**, L29-L32.
178. O. Vermesh, A. Aalipour, T. J. Ge, Y. Saenz, Y. Guo, I. S. Alam, S.-M. Park, C. N. Adelson, Y. Mitsutake, J. Vilches-Moure, E. Godoy, M. H. Bachmann, C. C. Ooi, J. K. Lyons, K. Mueller, H. Arami, A. Green, E. I. Solomon, S. X. Wang and S. S. Gambhir, *Nat Biomed Eng*, 2018, **2**, 696-705.
179. T. H. Kim, Y. Wang, C. R. Oliver, D. H. Thamm, L. Cooling, C. Paoletti, K. J. Smith, S. Nagrath and D. F. Hayes, *Nature Communications*, 2019, **10**, 1478.
180. J. Xie, Y. Gao, R. Zhao, P. J. Sinko, S. Gu, J. Wang, Y. Li, Y. Lu, S. Yu, L. Wang, S. Chen, J. Shao and L. Jia, *Journal of Controlled Release*, 2015, **209**, 159-169.
181. J. Xie, J. Wang, H. Chen, W. Shen, P. J. Sinko, H. Dong, R. Zhao, Y. Lu, Y. Zhu and L. Jia, *Scientific Reports*, 2015, **5**, 9445.